Trinity College Dublin
Coláiste na Tríonóide, Baile Átha Cliath
The University of Dublin

The treatment of obesity using magneto -mechanical effect

Chen Yangtianyi

Student No: 22321920

Project Supervisors:

Prof. Maria José Santos-Martínez and Dr. Oliviero Gobbo

Thesis submitted to the School of Pharmacy and Pharmaceutical Sciences, Trinity College Dublin, for the fulfilment of the degree of M.Sc. by Research in Pharmaceutical Sciences April 2024.

I declare that this thesis has not been submitted as an exercise for a degree at this or any other university and it is entirely my own work.

I have read and I understand the plagiarism provisions in the General Regulations of the University Calendar for the current year, found at: http://www.tcd.ie/calendar.

I have also completed the Online Tutorial on avoiding plagiarism 'Ready, Steady, Write', located at https://www.tcd.ie/library/support/plagiarism/story_html5.html.

I agree to deposit this thesis in the University's open access institutional repository or allow the Library to do so on my behalf, subject to Irish Copyright Legislation and Trinity College Library conditions of use and acknowledgement.

Signed_____

Chen Yangtianyi

Abstract

Obesity is a very prevalent condition that can be very often associated with the development of comorbidities, such as insulin resistance, hypertension, and hyperlipidaemia that can lead to cardiovascular and cerebrovascular diseases. The aetiology of obesity is multifactorial and may include overeating, hormonal dysregulation and genetic and psychological factors. It is associated with the presence of hypertrophy and hyperplasia of dysfunctional adipocytes, but its pathogenesis and related complications, have close connections with other cells in adipose tissue (AT), such as macrophages. Nowadays, treatment approaches include diet, exercise, drugs or surgery. However, although the former two approaches devoid of adverse effects, they are difficult to adhere to and obesity is therefore easy to rebound. On the contrary, the latter two, while quite effective, carry the inherent risk of complications that can even be life-threatening.

As a branch of nanotechnology, magnetic nanoparticles (MNPs) have undergone extensive development and bearing significant relevance in the realms of science and medicine. Due to their distinctive magnetic properties, MNPs can be detected and manipulated using remote magnetic fields. They have been applied in vitro for separation and purification, immunoassay, catalysts, and magneto relaxometry. In vivo, MNPs are utilized not only for therapeutic purposes, such as during hyperthermia and as drug carriers, but also in diagnostic applications using Magnetic Resonance Imaging.

The experimental focus of this study is on the use of a technology known as Nanomechanical Magnetic Activation. This technology involves the application of low-frequency alternating magnetic fields on MNPs to induce cell damage. We aim to apply this technology to treat obesity by targeting adipocytes. The main objective of this project was to investigate the effect that MNPs could exert on adipose tissue, in particular macrophages, when treated by this technology. During this project the potential toxic effect of MNPs with different surface coatings, which is crucial for the future development of nanotechnology, was investigated on macrophages, platelets and red blood cells. In the investigation of platelets and red blood cells, no significant potential interactions were observed between MNPs with three different surface coatings and platelets at the tested concentrations, and only one of the MNPs had an impact on red blood cells at high

concentrations.

The experimental results show that, as expected, MNPs were internalised in macrophages, as demonstrated by transmission electron microscopy, and that Nanomechanical Magnetic Activation is an effective method, to induce death cell in macrophages. Therefore it is highly urgent to further accelerate research on the surface coatings of MNPs to address different scenarios.

Table of Contents

Abbreviations

AEPA	6-Aminohexylphosphonic Acid
AT	Adipose Tissue
ATM	Adipose Tissue Macrophages
BAT	Brown Adipose Tissue
BMI	Body Mass Index
DLS	Dynamic Light Scattering
DMSA	meso-2,3-Dimercaptosuccinic Acid
EPR	Enhanced Permeability and Retention
HSP	Heat Shock Protein
LFAMF	Low-Frequency Alternating Magnetic Fields
LPS	Lipopolysaccharide
MTH	Magnetic Targeted Hyperthermia
MMPs	Matrix Metalloproteinases
MNPs	Magnetic Nanoparticles
MSCs	Mesenchymal Stem Cells
NMMA	Nanomechanical Magnetic Activation
NPs	Nanoparticles
PAA	Polyacrylic Acid
PBS	Phosphate Buffered Saline
RBCs	Red Blood Cells
WAT	White Adipose Tissue
VEGF	Vascular Endothelial Growth Factor
VLCKD	Low-Calorie Ketogenic Diets

1. Introduction

1.1 Obesity

Obesity is a chronic metabolic disease caused by many factors[1], typically developed when an energy imbalance occurs, leading to an excess of energy intake relative to energy consumption. This imbalance results in the excessive accumulation of body fat, especially triglycerides, further inducing hypertrophy and hyperplasia of adipocytes.

The human body fat is classified into subcutaneous fat and visceral fat (Figure1). Excessive accumulation of both types of fat can lead to obesity. The subcutaneous fat is situated beneath the skin, mainly distributed in areas such as arms, thighs, hips, and waist and that can be 'felt by hands'. It serves as the main storage site for energy in the human body and it has a strong capacity for fat storage. Enhanced triglyceride storage can be attained by hypertrophy and hyperplasia of adipocytes and fostering the angiogenesis[2]. In contrast, visceral fat is located deep within the body, coating or filling crucial organs including heart, liver, kidneys, and the gastrointestinal tract. The visceral fat has a smaller storage capacity relative to subcutaneous fat. Under physiological conditions, visceral fat functions protecting internal organs and mitigating damage caused by interorgan friction.

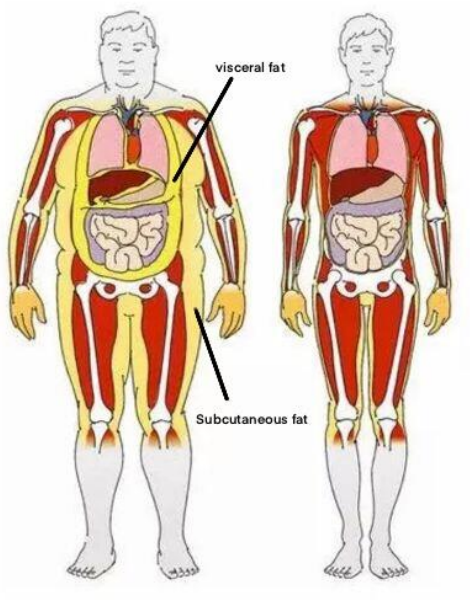

Figure 1: When obesity occurs, both subcutaneous and visceral fat in the human body increase significantly, especially subcutaneous fat. (http://mt.sohu.com/20180316/n532692676.shtml)

The excessive accumulation of fat within adipose tissue (AT) leads to the dysfunction of the adipose tissue and the consequent development of adiposopathy. It is noteworthy that, due to the impaired metabolic capability of adipocytes, they exhibit a failure to respond properly to most of the extracellular signals, such as insulin leading to the development of type 2 diabetes. At the same time, the adipocyte's dysfunction may induce the onset of chronic inflammation within the AT, making those individuals more susceptible to the development of hyperlipidaemia and hypertension, and therefore to cardiovascular diseases, in addition to an elevated risk of cancer.[3]

Body Mass Index (BMI) serves as a medical screening tool employed to evaluate an individual's weight status in terms of health. BMI is calculated by dividing weight in kilograms or pounds by height in meters or inches squared (Figure 2). Typically, a high BMI is associated with a higher proportion of body fat, where values exceeding 30 imply obesity. Nevertheless, BMI does not measure body fat directly. As an indirect marker of obesity, it has numerous limitations, as it does not consider factors such as age, gender, bone structure, fat distribution or muscle mass. For example, in some fitness enthusiasts, their high muscle density can lead to a higher BMI compared to the normal. However, this does not imply that they are obese.[4].

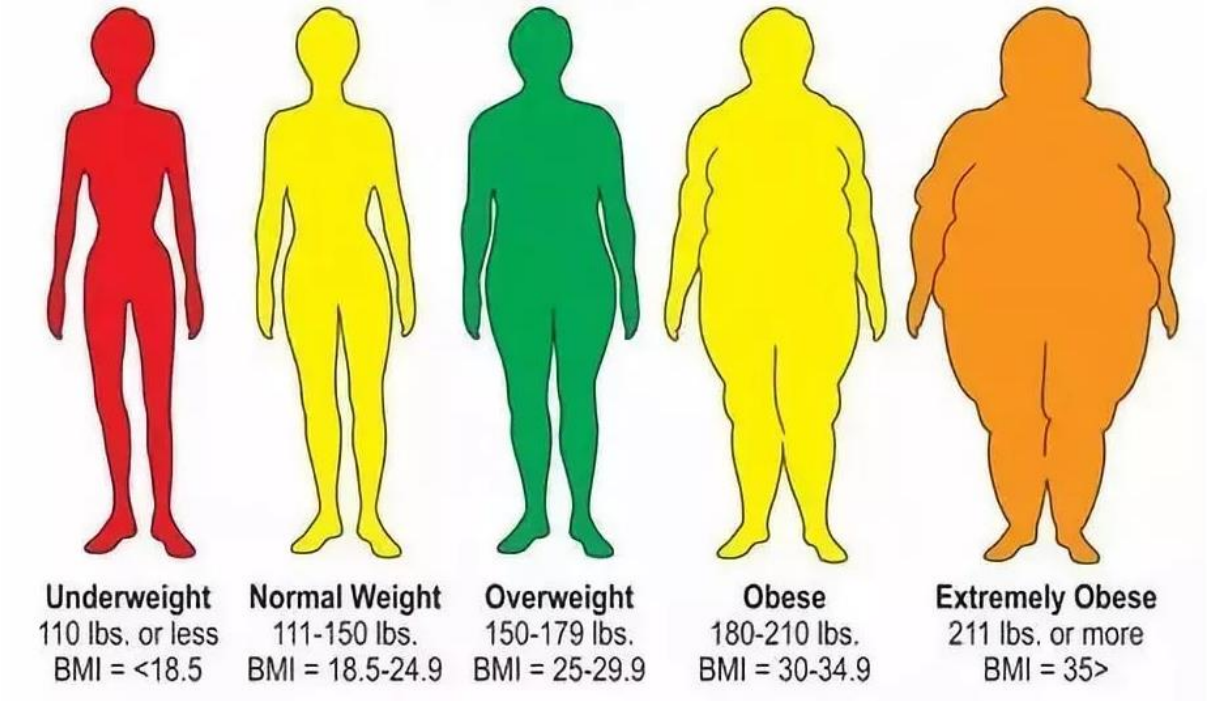

Figure 2: Graphical representation of the relationship between BMI and human body shape. (http://mt.sohu.com/20180530/n539248839.shtml)

In addition to BMI, other several comprehensive methods are available for assessing the presence of obesity. Skinfold thickness measurements, conducted with a caliper at various points such as the triceps and below the scapula, can measure subcutaneous fat; 10mm-40mm for men and 20mm-50mm for women are normal. Waist circumference measurements ascertain the diameter at the midpoint between the anterior superior iliac spine and the lower 12 costal margins, with normal values typically falling below 85cm for men and 80cm for women. The waist-to-hip ratio offers another method to estimate obesity. It is calculated by comparing the circumference of the waist to the circumference of the most prominent point of the pelvis, around the buttocks, or hip circumference. Usually, a ratio below 0.9 for men and below 0.85 for women is considered normal. Moreover, the degree of obesity can be assessed using body density and bioelectrical impedance measurements. More scientifically accurate measurement methods by using advanced imaging techniques, such as computerized tomography (CT) scans and magnetic resonance imaging (MRI), can also be utilized to determine body fat content[5].

1.1.1. Adipose tissue

Adipose tissue (AT) is composed by adipocytes and the stromal vascular cells that include preadipocytes, adipocytes, fibroblasts, macrophages and monocytes together with vascular and innervation cells. However, by extracting fat tissue DNA, it has been determined that 80% of the cells in the normal AT are vascular cells, fibroblasts, leukocytes and macrophages[6]. During the development of obesity, almost all known immune cell types can be found in AT, including macrophages, T cells (CD4, CD8, Tregs), B cells, natural killer T cells, dendritic cells, neutrophils, eosinophils, and mast cells.

In general, the AT environment becomes more ‘inflammatory’ during the transition from the lean to the obese state[7]. Macrophages, as resident immune cells in AT, play a crucial role in regulating the homeostatic environment of normal AT and are also involved in

modulating the metabolic dysregulation that takes place in obesity. Numerous studies focused on mice and humans have characterized the mechanisms by which immune cell populations contribute to obesity-related inflammation and metabolic dysfunction[8].

In the human body, there are three types of adipocytes: white adipocytes, brown adipocytes, and beige adipocytes. White adipocytes exhibit a larger volume compared to brown adipocytes and have few organelles in their cytoplasm accounting for only 15% of their total cell volume. A large lipid droplet occupies the central region of the cell, constituting 85% of the cell volume and displacing the nucleus to the periphery. The main function of the white adipose tissue (WAT) is to store fat in the form of triglycerides and to release free fatty acids (FFA) during periods of starvation or energy demand. In the context of rapid obesity development, white adipocytes undergo hypertrophy, while in cases of prolonged, gradual obesity, their numbers also increase. Brown adipocytes have smaller and more dispersed lipid droplets in the cytoplasm and are enriched with numerous mitochondria. They possess the ability to burn fat and generate heat, contributing to thermogenesis. Beige adipocytes, are mainly distributed in the regions of WAT, however, from the morphological point of view, they are more similar to brown adipocytes and are characterized by having small and more lipid droplets and numerous mitochondria. White adipocytes can undergo differentiation into beige adipocytes in response to cold exposure and exercise stimuli. Importantly, this process is reversible, and beige adipocytes can revert to white adipocytes when the temperature returns to normal[6] (Figure 3).

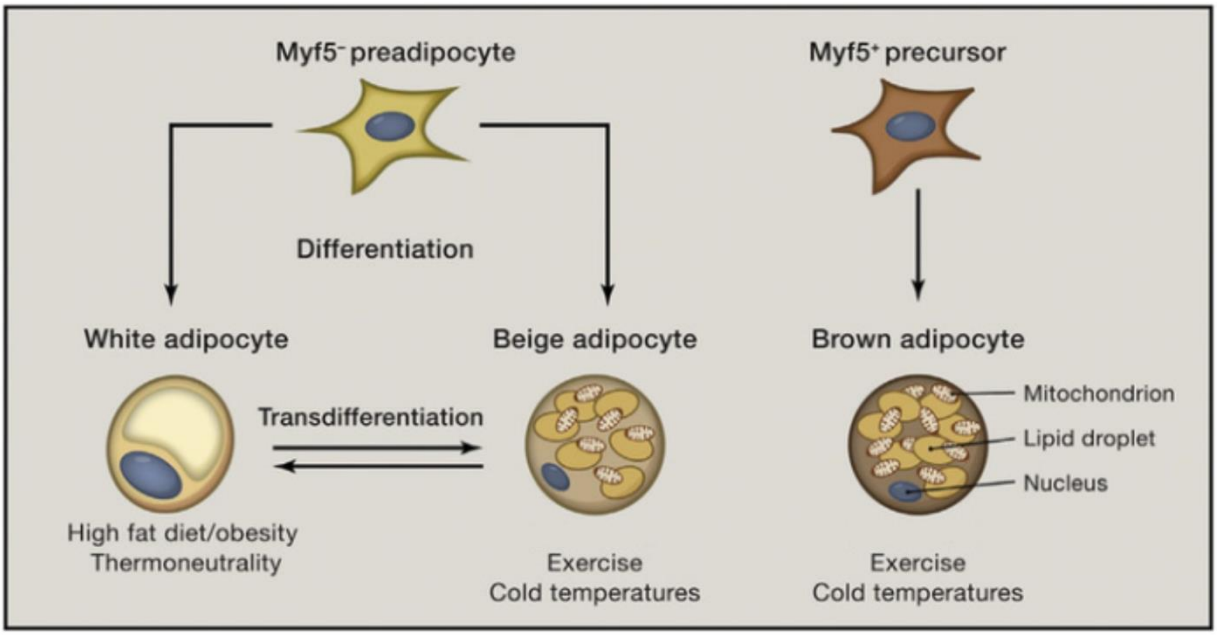

Figure 3: Structures and transdifferentiation of the different adipocyte types. [9]

Some studies have identified macrophages as crucial participants in the formation and activation of beige adipocytes. For instance, it has been demonstrated that pro-inflammatory macrophages directly interact with beige adipocytes through α4 integrin and VCAM-1, triggering a sustained inflammatory cycle in AT and suppressing the generation of beige adipocytes in obesity. Conversely, anti-inflammatory macrophages contribute to beige adipocyte formation through the cytokine Slit3[10]. Adipose tissue macrophages (ATMs) remain as a critical factor contributing to local and systemic inflammation in obesity. During obesity pro-inflammatory macrophages accumulate in AT releasing a wide variety of cytokines such as TNF-α, IL-6, and IL-1β. It has been demonstrated, for example, that IL-1β mediates, to some extent, insulin signalling in human adipocytes[11]. Research has indicated that the inhibition of Dipeptidyl Peptidase-4 (DPP-4) by sitagliptin reduces obesity-related insulin resistance and inflammation by modulating the macrophage polarization[12].

Therefore, although further research is needed, ATMs might represent a potential strategy for the treatment of obesity.

1.1.2. Obesity: prevalence, aetiology, and its associated health risks

As the pace of technological progresses and the development of social economy increases, the overweight and obesity rate of adults and children continues to rise worldwide. In fact, according to the World Health Organization, in 2016, 39% of adults aged 18 years and over (39% of men and 40% of women) were overweight. Between 1975 and 2016, the global prevalence of overweight or obesity among children and adolescents (aged 5-19) increased more than fourfold, from 4% to 18%[13]. Based on the 2017-2018 American National Health and Nutrition Examination Survey, 30.7% of American adults were

classified as overweight, more than 42.4% were considered obese, and about 9.2% were classified as severely obese[14]. According to Eurostat, as of 2019, 52.7% of adults (aged 18 and over) in the European Union and regions such as Norway, Serbia and Turkey were overweight[15].

For instance, many individuals have changed their mealtime due to their work. This often results in the necessity to compress or postpone mealtimes or, in some cases, forego formal meals altogether. There is also a tendency to choose fast food or processed food, which has been linked to long-term weight gain and obesity[1]. The escalation of obesity rates is also notable among children and adolescents, who tend to have less self-control and, as a result, may eat too much. Furthermore, they are also more likely to be attracted by the palatability of fast food and processed food items[16].

Among those individuals grappling with obesity, a recurring pattern emerges wherein they tend to consume substantial quantities of food, particularly those high in calories, carbohydrates and fats. Additionally, late-night eating is a common practice among this group. These dietary habits, coupled with a lack of physical activity, result in an energy surplus within the body, ultimately leading to the development of obesity. Nonetheless, it's important to recognize that obesity doesn't always stem from dietary habits and physical inactivity alone. In some cases, there is a genetic predisposition, and obesity can be associated as well to circumstances that are beyond the individual's direct control[1]. For instance, prolonged periods of bed rest following surgical procedures can lead to weight gain due to limited calorie expenditure resulting from restricted mobility. Furthermore, the use of certain drugs such as hormone-based medications, antipsychotics and antidepressants can also contribute to obesity, attributed in these instances to disruptions in the regulation of fat and carbohydrate metabolism by the neuroendocrine system[17].

The most obvious manifestations of obesity are weight gain and an increase in body size where fat accumulates in regions characterized by greater adipose storage, such as the neck, torso, and abdominal areas. In cases of more severe obesity, individuals may develop heat intolerance, reduced mobility, snoring during sleep, and breathlessness during physical activity. When following the same dietary intake, obese individuals tend to have a higher anabolic rate than those with normal weight. Furthermore, they spend less energy while at rest or during moderate physical activities. In a sedentary state, obese individuals also

display a diminished response to cold and do not experience the same increase in metabolic rate when needed as non-obese individuals[18]. Obesity can also give rise to psychological issues. Many patients with obesity grapple with profound shame stemming from their body shape, occasionally leading to feelings of self-loathing. Consequently, these emotions can contribute to the development of psychological issues, including negative moods, anxiety, and depression. For some, these psychological issues may impact their daily lives, occasionally leading to the emergence of somatic symptoms like headaches, stomach discomfort, and insomnia, among others[19]. In essence, the clinical manifestations of obesity extend beyond the physical domain, encompassing a spectrum of physiological, psychological, and emotional issues that underscore the multifaceted nature of this health concern.

Although it is widely recognised that obesity frequently leads to hypertension, diabetes, and dyslipidaemia, heightening the risk of cardiovascular diseases, it is worth mentioning that there are other conditions and diseases associated with obesity. For example, as the liver serves as the site for triglyceride synthesis, their accumulation in this organ contributes to the development of fatty liver disease[19]. Obesity also has a substantial impact on the respiratory system. Individuals with obesity experience excessive fat deposition in the neck region, resulting in ‘constriction’ of the upper respiratory tract. This can just lead to snoring or in some cases progress to Sleep Apnoea Syndrom, characterised by intermittent episodes of 'temporary cessation of breathing during sleep'[20]. Another respiratory ailment linked to severe obesity is Pickwick syndrome. In this condition, the excessive AT in the abdominal and chest cavities restricts respiratory movements, resulting in poor pulmonary ventilation. This leads to the retention of carbon dioxide, which, when surpassing the normal range, leads to respiratory acidosis[21, 22].

As previously mentioned, ATMs are recognised as crucial factors in triggering inflammation in obesity. Macrophages are generally categorised into two main phenotypes: M1 and M2. M1 macrophages are in charge of phagocytosing and clearing foreign pathogens, secrete pro-inflammatory cytokines, activate T-cell immune responses, and promote early-stage inflammatory reactions. On the other hand, M2 macrophages primarily participate in anti-inflammatory responses, facilitating tissue repair and wound healing and in the later stages of inflammation, contribute to disease recovery. In the context of obesity in AT, ATMs tend to polarise towards M1 macrophages, disrupting the

balance between pro-inflammatory and anti-inflammatory responses [23]. ATMs present in the tumour microenvironmen, have been also involved in tumour growth, metastasis, angiogenesis, and immune evasion of adipose-related malignancies. Obesity induces a metabolic and phenotypic reprogramming of ATM. For instance, the increased incidence of Triple-Negative Breast Cancer is associated with obesity and it is hypothesised that obesity reprograms macrophages in mammary AT to adopt a pro-inflammatory metabolic phenotype, altering the niche to support tumorigenesis[24].

While macrophages also release a significant substance, Matrix Metalloproteinases (MMPs). This is a protein released by various connective tissues and pro-inflammatory cells, playing a crucial role in cell proliferation, angiogenesis, and apoptosis[25]. Among them, MMP-2 and MMP-9 belong to the gelatinase category and their levels can be detected through enzymatic assays, allowing for in-depth investigation. Both MMPs are closely associated with pro-inflammatory macrophages linked to inflammation, especially in the occurrence of obesity, where macrophages tend to polarise towards M1 phenotype. Studies also suggest the involvement of MMP-9-related vascular endothelial growth factor (VEGF) in angiogenesis during obesity[26].

The aetiology of obesity is diverse, encompassing a spectrum of specific conditions and the intricate interplay of lifestyle choices. The physiological and psychological impacts resulting from obesity are complex. Understanding the factors involved in the development and maintenance of the disease and its consequences, including the role of macrophages in obesity, is of paramount importance for devising effective strategies to address and combat this complex disease.

1.2 Nanotechnology and medicine

Nanomaterials and nanotechnology emerged in the 1990s as new fields, representing another industrial revolution following the internet and genetic technology. Nanomaterials

serve as the foundation of nanotechnology and hold significant potential for applications in various domains, including information technology, biology, energy, and environmental science. Nanotechnology in medicine, referred to as nanomedicine, can contribute to both diagnostic and therapeutic applications. The integration of nanotechnology in medicine has driven advancements in fundamental medical research, clinical diagnostics, and treatment modalities, such as the utilization of nanotechnology in tissue repair and regenerative medicine.

Engineered nanomaterials are defined by having at least one dimension that is less than 100 nm in size[27]. However, within the field of medical science, particles with larger dimensions (even microns) are very often referred to as nanoparticles (NPs). These NPs can be of organic nature, including lipids and biopolymers, or inorganic, consisting of materials like metals, oxides, and carbon. Additionally, they can be designed with various shapes, such as cubes, stars, spicules and other complex geometries[28].

Nanotechnology has found extensive applications in the field of medicine, particularly in the realm of 'detection technology'. For example, in the 1980s, nano SiO_2 was employed for cellular separation[27]. In this method, SiO_2 particles with sizes ranging from 15 to 20 nm were uniformly dispersed in a polyethylpyrrolidone solution containing various types of cells and they were swiftly separated using centrifugation based on the gradient principle. This technique has been implemented in clinical medicine and can be utilized, for instance, to isolate foetal cells obtained from pregnant women, enabling the assessment of genetic defects through chromosome analysis[29]. In common diagnostic techniques such as Computed Tomography (CT) and Magnetic Resonance Imaging (MRI), it is typical to inject contrast agents into the patient's body to significantly enhance imaging resolution. Some NPs even exhibit a propensity to aggregate around tumour cells, which can be exploited for early tumour detection. For instance, there is a type of iron (III) oxide nanoparticle measuring 5 to 10 nm in size that coated with a hydrophilic material, it tends to accumulate in liver tumours. This accumulation alters the spin of water protons, enhancing the imaging effect and aiding in the early diagnosis of this type of tumours using MRI[30, 31].

NPs can be categorized into two primary types: organic and inorganic NPs. Among the organic NPs, lipid-based structures are the most widely used. They have a spherical form, composed of one or more lipid bilayers and offer several advantages as delivery systems, including formulation simplicity, self-assembly, biocompatibility, high bioavailability, the capacity to carry substantial payloads, and the ability to control various physicochemical properties to modulate their biological characteristics. As a result, lipid-based NPs represent the most common class of FDA-approved nanomedicines[32]. Inorganic materials, such as gold, iron, and silica, have been also employed to create nanostructured materials for both, drug delivery and imaging applications. These inorganic NPs can be tailored in terms of size, structure, and geometry. Due to their magnetic, radioactive, or plasmonic attributes, inorganic nanoparticles are exceptionally suited for applications such as diagnostic imaging, and photothermal therapies. Most of them exhibit good biocompatibility and stability, filling in the unique properties that organic materials may not provide. Nevertheless, there are still some NPs in development that, due to issues related to low solubility or toxicity, cannot be utilized in clinical applications, particularly those NPs incorporating heavy metal particles[32].

The most common application of nanotechnology in medicine revolves around cancer treatment using NPs. These NPs can accumulate in tumours through passive or active targeting mechanisms[33]. The distinctive interactions and diverse processing pathways of NPs enhance their targeting ability, allowing for the discrimination between pathological and normal tissues. Furthermore, they offer the advantage of adjustable drug composition and proportions depending on the specific circumstances.[34]. Typically, these nanoparticles exhibit passive targeting towards specific organs and can traverse tissue endothelial cells to reach malignant tumour cells. This phenomenon is commonly referred to as the Enhanced Permeability and Retention (EPR) effect, denoting that alterations in vascular permeability enable specific particles to exhibit a greater tendency to infiltrate tumour tissue. This phenomenon is secondary to the development of new blood vessels associated with tumour expansion, which, in comparison to normal vasculature, present wider interstitial gaps, reduced structural integrity, and inadequate lymphatic drainage. These characteristics facilitate the traversal of relatively large macromolecules and lipid particles through the vessel walls of these neovascular structures, allowing them to enter

the surrounding interstitial fluid. Enhanced vascular permeability and increased permeability for macromolecules can create favourable conditions for tumour growth, as they accumulate within nutrient-deprived tumour tissue, promoting tumour proliferation. However, drugs that access tumour tissue through this mechanism can also be retained for extended durations to exert their therapeutic effects[35, 36].

1.2.1. Magnetic nanoparticles

Magnetic nanoparticles (MNPs) have a series of unique and superior physical and chemical properties. With the development of synthesis technology, a series of magnetic nanoparticles with controllable shape, good stability and mono dispersion has been successfully produced. Their magnetic properties make them easy to be clustered together, separated, and oriented to move and locate. MNPs exhibit favourable biocompatibility and can be functionalised with a wide range of non-polymeric organic substances, polymeric organic compounds, inorganic molecules, and materials tailored for specific targeting purposes[37]. Commonly employed substances for MNPs' modification include glucan, polyvinylpyrrolidone, fatty acids, polyethylene glycol, polyethylene ethanol, polypeptides, chitosan, and methyl silane. Two approaches are primarily used for this purpose 1) chemical bonding of small organic molecules to the material and particle surface 2) direct coating of MNPs with organic or inorganic materials, encompassing surfactants, polymers, precious metals, and silica. Surface modification serves for multiple purposes, including: enhancing stability, improving dispersibility in aqueous solutions, enhancing targeting capabilities, preventing protein adsorption, prolonging their circulation time in the bloodstream, improving their biocompatibility and enabling further conjugation with other nanoparticles, compounds, or biological ligands[38].

Iron, cobalt, nickel, and various crystalline materials exhibit ferromagnetism. However,

due to the high biological safety of iron oxide magnets, the most magnetically potent natural minerals on Earth, and the pronounced biological toxicity associated to cobalt and nickel materials, superparamagnetic iron oxide MNPs are preferred for biomedical applications. Nonetheless, the potential toxicity effect of MNPs cannot be always granted [39], due to their capacity to accumulate within cells and to trigger organ-specific effects. Upon introduction into the body and subsequent circulation in the bloodstream, MNPs can distribute and accumulate within various organs, including the liver, spleen, lungs, and kidneys. Some investigations have even suggested that MNPs may accumulate in the brain, particularly if their size is less than 10nm or if there are breaches in the body's blood-brain barrier. Furthermore, MNPs' accumulation may influence their biological distribution and organ deposition. Recent studies employing various animal models have illustrated MNPs accumulation in different organs, interaction with cellular macromolecules, and the induction of oxidative stress. Mechanisms underlying MNPs toxicity in target organs encompass the generation of reactive oxygen species, DNA damage, alteration of protein structure and functionality, and disruption of membrane integrity [40].

Strategies to mitigate cytotoxicity typically involve the application of various coatings. In fact, while uncoated iron oxide nanoparticles exhibit some toxic effects, it has been demonstrated that coated MNPs tend to have relatively low toxicity. Gupta et al. demonstrated that cells exposed to Polyethylene glycol (PEG)-coated MNPs retained over 99% of their activity compared to the control group at high concentrations (1 mg/mL). Conversely, they noted that the cytotoxicity of MNPs showed a dose-dependent relationship, resulting in approximately a 60% reduction in cell viability when the concentration was raised to 2 mg/mL[39]. However, in studies employing different PEG-based coatings, Yu et al. reported that MNPs coated with poly (maleic anhydride-alt-1-octadecene)-Polyethylene glycol (PMAO-PEG) exhibited relatively low toxicity, causing only a 9% reduction in cell viability following exposure to MNPs[41, 42].

1.2.2. Applications of MNPs

The most significant characteristic of MNPs is their capacity to interact with a magnetic field. Present applications of MNPs encompass magnetic separation techniques, their deployment as diagnostic instruments, agents for drug delivery, and as direct therapeutic agents.

In biomedical research, the separation of RNA/DNA, proteins, and cells serves as an essential prerequisite for the advancement of biotechnological applications across various domains within the life sciences. In this regard, due to their distinctive physical and chemical properties, MNPs have the capacity to streamline complex conventional experimental procedures, thereby reducing experimental time. Among the various biological separation techniques, MNPs offer a compelling approach for biological separation based on their unique magnetic separation effect and promising efficiency. This concept has been extensively documented in the literature and has found widespread applications. Biological molecules can be labelled with colloidal MNPs, and separation achieved under the influence of an externally applied magnetic field. This technique can be applied across diverse domains, including cell separation, protein purification, RNA/DNA extraction, and immunoprecipitation. Magnetic beads and similar magnetic nanoparticles, characterized by their small size, superior separation efficiency, and excellent dispersibility, have been widely employed for the isolation and purification of cells and biomolecules. A noteworthy trend in the advancement of this field involves the utilization of antibodies coupled with magnetic beads for magnetic separation, thereby enabling highly precise separation through the specific binding of antibodies to corresponding antigens located on the targeted surface[43].

The utilization of MNPs as diagnostic tools facilitates their application in cell labelling and the development of non-invasive imaging techniques. Among these techniques, MRI stands out as a widely adopted diagnostic tool, owing to its ability to deliver high spatial resolution and detailed anatomical information. Several varieties of magnetic nanoparticles have been devised to enhance the performance of contrast agents in MRI imaging, offering notable advantages such as increased sensitivity and detection at moderate concentrations, along with favourable biocompatibility. Traditional inorganic NPs, like gold NPs and quantum dots (QD), which are capable of detecting numerous cancer biomarkers in blood assays or cancer tissue biopsies, have demonstrated promising outcomes in animal models but do not find practical application in clinical in vivo diagnostic imaging[44]. In contrast, MNPs have already established themselves in clinical practice as MRI contrast agents. Currently, two distinct categories of MNPs are employed for clinical imaging: ferromagnetic iron oxide particles and ultrasmall superparamagnetic iron oxide particles[45].

The current therapeutic applications of MNPs are primarily around cancer treatment. In conventional cancer treatment, cytotoxic drugs are typically administered intravenously and systemically distributed. However, this non-specific approach leads to significant side effects as these drugs will affect not only tumour cells, which are the primary target, but also healthy normal cells. MNPs can serve as valuable tools for cancer treatment as nanocarriers that can enable controlled drug release specifically at the tumour site, facilitating hyperthermia treatment or as a combination of both strategies. The targeted delivery of anti-tumour drugs adsorbed onto the surface of MNPs represents a highly promising alternative to traditional chemotherapy. In this approach, particles loaded with drugs are concentrated at the target site with the assistance of external magnets and subsequently released into the desired area[46].

After an extensive period of technological advancement, magnetic technology has seamlessly integrated with nanotechnology, and numerous studies have showed its remarkable efficacy in targeted cancer therapy. Lin Chen et al. conducted a randomized experiment using adriamycin and n-butyl poly cyanoacrylate as therapeutic agents and carriers, respectively, in a human liver cancer model established in nude mice[47]. The experimental outcomes demonstrated that the therapeutic efficacy of the treatment significantly surpassed that of other groups when magnetic field-guided drug-loaded nanoparticles were employed. Moreover, the pathological sections from the treated group exhibited the most pronounced tumour cell necrosis. These findings emphasize the excellent targeting capability and effective anti-cancer potential of MNPs under the influence of an external magnetic field. The incorporation of monoclonal antibodies onto MNPs allows them to specifically bind to the receptor of interest with high selectivity, potentially enhancing drug efficacy and mitigating toxic side effects. Yu Dexin et al. coated MNPs with a biocompatible polymer material (polylactic acid - polyethylene glycol polylysine) and immobilized Vascular Endothelial Growth Factor (VEGF) antibodies onto the surface of the carriers and subsequent experimental results, confirmed by MRI scans, supported the effectiveness of this approach[48]. Chen et al. developed monoclonal antibody magnetic nanoparticles specifically designed for targeting hepatocellular carcinoma (HCC) tumour cells. These NPs were subjected under the influence of a magnetic field, leading to significant achievements and offering a promising alternative therapeutic approach for HCC[48].

Nanomechanical Magnetic Activation (NMMA) represents a distinct category of techniques that involve the nanoscale deformation of molecular structures using MNPs activated by non-heating low-frequency (LF) alternating magnetic fields (AMF). These techniques have been developed over the past two decades. NMMA capitalizes on the sensitivity of tissues, cells, vesicles, and micelles to the applied force and induced deformation. Thus, altering the mechanical homeostasis within the organism, guiding cellular apoptosis. The utilization of mechanotransduction has opened vast prospects for the development of new methods and technologies in the fields of tumour therapy, neurodegenerative diseases, regenerative medicine, and other biomedical disciplines. There is evidence to suggest that in certain situations, low-frequency alternating magnetic fields (LF-AMF) can induce biophysical effects in organisms, tissues, and cells lacking MNPs, but the efficiency is low. However, if MNPs are introduced, greater forces are generated, significantly enhancing efficiency[49].

Experimental evidence has demonstrated that the activation of MNPs through non-heating AMF at frequencies ranging from 10 to 50 Hz can alter enzyme activity and enhance vesicles and cell membranes permeability. This phenomenon might offer a novel therapeutic approach, especially for large cells like adipocytes. During NMMA treatment, modifying the permeability of adipocyte membranes could potentially lead to the release of stored triglycerides. By discontinuing the magnetic field after treatment, it becomes possible to address obesity without damaging the adipocytes themselves. This approach presents a promising avenue for obesity treatment[49].

2. Aims

Obesity is a very prevalent disease, and it is associated to multiple health conditions. Current treatments are not as effective as desired or may be associated to severe side effects. Therefore, research for developing new approaches for tackling obesity is needed. The main objective of this research is to investigate a different approach for the treatment of obesity using NMMA.

This project focuses on the effect that MNPs and the application of the LF-AMF may exert on macrophages, as they are one of the most abundant cells in the AT and important players in adiposopathy during the development of obesity.

The specific aims of this research are:

- To characterise the MNPs tested (size, charge and biocompatibility)
- To assess the blood compatibility of the MNPs ex vivo using red blood cells and platelets isolated from human blood.
- To evaluate the potential toxic effect of the MNPs on macrophages in vitro.
- To evaluate the effect of the low frequency alternating magnetic field on macrophages in the presence and absence of MNPs.
- To investigate gelatinase activity from macrophages incubated with MNPs and expose to the low frequency alternating magnetic field.

3. Materials and Methods

3.1. Reagents

All reagents used were purchased from Sigma Aldrich (Merck Life Science, Ireland) unless otherwise stated.

3.2. Magnetic nanoparticles

The magnetic nanoparticles used during this project were synthesized in the Institute of Chemistry of OrganoMetallic Compounds in Florence (Italy) by Dr Claudio Sangregorio Research team. The MNPs were coated with meso-2,3-dimercaptosuccinic acid (DMSA), polyacrylic acid (PAA) or 6-aminohexylphosphonic acid (AEPA)(In the following, PAA, DMSA and AEPA will refer to the three different surface coated MNPs.) (Figure 4)

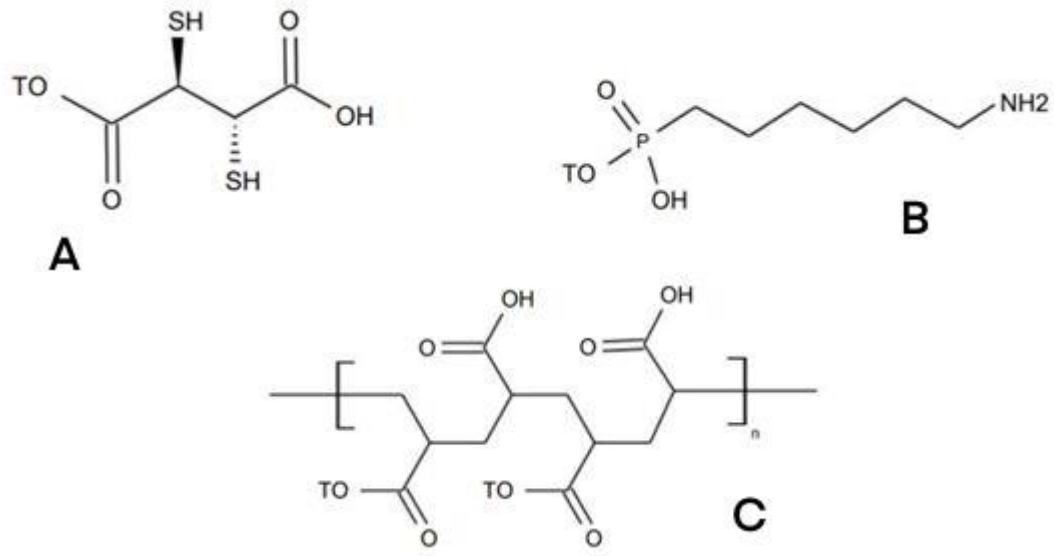

Figure 4: Schematic representation of the three cappants used in this thesis work. A) meso-2,3-dimercaptosuccinic acid (DMSA); B) 6-aminohexylphosphonic acid (AEPA) and C) polyacrylic acid (PAA).

MNPs were characterise in house upon arrival and under different conditions. Size and zeta potential were measured using a Zetasizer Nano (Malvern Pananalytical, UK). Particle size was determined by Dynamic Light Scattering (DLS). DLS is utilized for the characterization of particles, emulsions, or molecules dispersed or dissolved in a liquid medium. The Brownian motion of particles suspended in a solution leads to fluctuations in the scattered light intensity. Analysing these fluctuations yields information about the Brownian motion velocity of particles, which can then be used to determine their size using the Stokes-Einstein equation[50]. Zeta potential is measured through Electrophoretic Light Scattering (ELS), a technique used to assess the electrophoretic mobility of dispersed particles or molecules in a solution. This technique operates on the principles of electrophoresis. A dispersed sample is placed within a sample cell containing two electrodes. When an electric field is applied through the electrodes, particles or molecules with a net charge, or more precisely, substances with a net electrophoretic potential, will move toward the electrode of opposite polarity at a rate correlated with their electrophoretic potential, also known as mobility[51].

The MNPs were first sonicated for 30 min, filtered (0.22µm) under sterile conditions and then diluted with different solutions (DMEM with 10% FBS, DMEM without FBS, water or PBS). Subsequently, an appropriate volume of the diluted liquid was introduced into a 12mm glass cell and a disposable folded capillary cell using a syringe (Figure 5). After covering the cells with their respective caps, they were placed into the instrument for measurement.

Figure 5: Square glass cell used for DLS (PCS8501, left) and disposable folded capillary cell used for ELS (DTS1070, right).

Note that for all experimental procedures, MNPs were always sonicated for 30 minutes prior to use.

3.3. Blood collection and platelets and red blood cells preparation

Blood samples were obtained from healthy volunteers who had abstained from taking any medications known to influence platelet function for a minimum of 14 days before blood collection. Ethic's approval for this study was obtained from the School of Pharmacy and Pharmaceutical Sciences Level 1 Research Ethics Committee (Trinity College Dublin; Reference No. of Study 2015-06-01 MS), following institutional guidelines and in accordance with the Declaration of Helsinki. All donors gave written informed consent, and were over the age of 18 years.

Whole blood was withdrawn and gently mixed in a falcon tube with a 3.15% sodium citrate solution (9:1 v/v ratio). Platelet rich plasma (PRP) and red blood cells (RBCs) were separated through differential centrifugation utilizing an Eppendorf 5804 centrifuge (Fisher Scientific, Ireland) at 250xg for 20 minutes at room temperature (Figure 6).

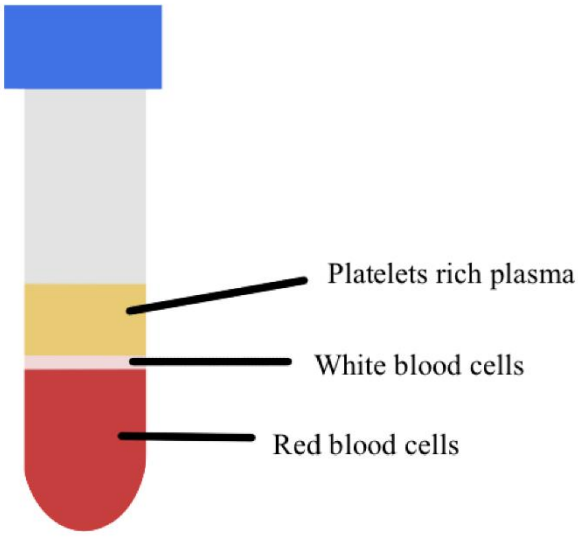

Figure 6: The upper yellow layer contains platelets and plasma (platelet rich plasma-PRP). The middle thin white layer contains white blood cells and the lowest dark red layer is composed mainly of red blood cells.

PRP was carefully collected, platelet concentration determined using a Beckman Coulter Z1 (Labplan, Ireland) and adjusted to 250,000 platelets/µL with Tyrode's buff. PRP underwent an additional centrifugation step at 900 xg for 10 minutes to obtain platelet-poor plasma (PPP).

For the preparation of RBCs, 1 mL was retrieved from the bottom of the falcon tube and mixed with 10 mL of 0.9% NaCl, followed by thorough mixing and centrifugation at 500xg for 5 minutes. The upper layer was discarded, and the RBCs were resuspended in NaCl at a 1:1 volume ratio and centrifuge again. This procedure was repeated twice using phosphate buffered saline (PBS). Finally, 1 mL of washed RBCs was diluted with 49 mL of PBS before use for haemolysis assays.

3.3.1. Haemolysis Assay

Haemolysis assays were performed to determine if the MNPs could affect RBCs' integrity. Disruption of RBCs, leads to the release of haemoglobin and other cellular contents into the surrounding environment. The extent of RBCs lysis can be measured by quantifying the haemoglobin (Hb) content in the sample using a spectrophotometer[52].

RBCs were subjected to various concentrations of MNPs (20, 50, 75, and 100 µg/µL) within a 96-well plate, following the layout shown in figure 7. Afterwards, the plate was kept at 37°C for 2 hours, subsequently subjected to centrifugation at 500xg for 5 minutes, and 100 µL of the resulting supernatant was transferred to another plate for absorbance measurement at 540 nm using a microplate reader, the measurements were taken in duplicated and averaged (BioTek Synergy H1 Multimode Reader, Agilent). The supernatant from RBCs that were not exposed to MNPs was employed as a negative control (Ctrl-), while the supernatant from RBCs exposed to Triton served as a positive control (Ctrl+; max. Hb release).

Figure 7: Layout of the experimental procedure for haemolysis. RBCs were treated with three types of MNPs (PAA, DMSA and AEPA) by duplicate in a 96-well-plate (The colour is used to indicate the different types of MNPs)

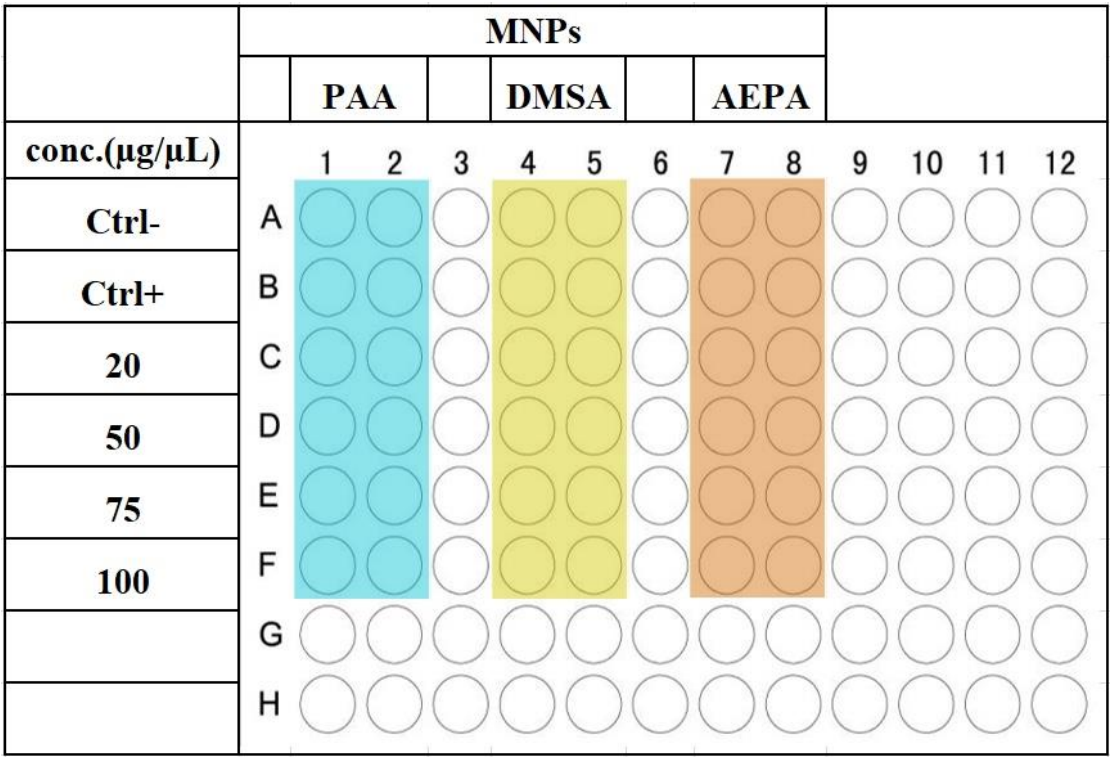

Following their incubation with MNPs, RBCs were fixed with paraformaldehyde to a final concentration of 2%, transferred into slides using a Cytospin 4 (Fisher Scientific, Ireland) and visualized using an Olympus BX51M optical microscope (Mason Technology, Ireland).

3.3.2. Light transmission aggregometry

The photometric turbidity method primarily relies on the light scattering properties of particles within a suspension. When light passes through the suspension, the extent of attenuation of the incident light is determined by the size or the quantity of particles in the suspension within the liquid. When testing platelet function using a photometric aggregometer, the optical density of stirred platelet suspensions is measured. PPP is used as the blank, set as 100% aggregation, and the percentage of aggregation is subsequently calculated based on the recorded changes in light transmittance (Figure 8)[50].

In this experiment, the potential aggregatory effect of the three types of MNPs was investigated using a PAP-8 (Platelet Aggregation Profile PAP-8E, Biodata Corporation, Ireland). For this purpose, platelets were incubated in the absence or presence of MNPs at different concentrations (20, 50, 75, and 100 µg/µL) for 60 minutes and the changes in light transmission recorded by the device for 60 minutes. Since MNPs themselves can

affect optical density, PPP containing the corresponding concentration of MNPs were used as blanks. Collagen at 5µg/mL was used to confirm that platelets were functional after preparation, Collagen was obtained from Chronolog (Labmedics, UK).

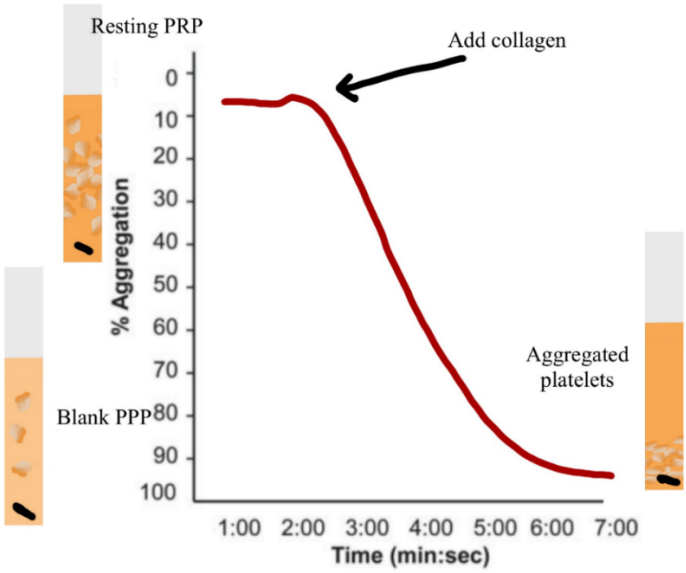

Figure 8: Platelet function was assessed using the light transmission aggregometry principle. (DOI: 10.1039/c1an15445a)

3.4. Cell Culture

Murine macrophages (RAW 246.7) were kindly donated by Prof Anna Laurenzana (University of Florence, Italy). Cells were cultured with Dulbecco's Modified Eagle Medium (DMEM) high glucose with 10% supplement of Foetal Bovine Serum (FBS) and subculture when 80% confluence was reached.

Cells were maintained in a humidified atmosphere in an incubator at 37°C and 5% CO_2 (Thermo Scientific, Ireland)

RAW 246.7 cells were treated with lipopolysaccharide (LPS) and provided by Bashaer Alsharif (research team colleague) to be used as positive control for gelatine zymography (section 3.9)

3.5. Cell viability

The cell viability of RAW 246.7 cells incubated with various concentrations of PAA was assessed after 24 hours and 48 hours of exposure using 24-well plates. Cells (50,000 cells/well) were seeded and incubated with complete culture medium (DMEM high

glucose with 10% FBS) for 24 hours. Afterwards, the media was replaced by DMEM high glucose with 0.5% FBS and kept for another 24 hours in the incubator prior to cell exposure to the PAA.

After 30 minutes of sonication, PAA were prepared at different concentrations (10, 25, 50, 75, 100 µg/mL) under three different conditions: 1) DMEM high glucose culture medium with 0.5% FBS, 2) DMEM high glucose culture medium with 10% FBS, or 3) DMEM high glucose culture medium without FBS. Subsequently, 1 mL of culture medium containing the corresponding concentration of PAA needed was added to each well. Each plate was divided into upper and lower sections with different FBS contents and incubated for 24 and 48 hours (Figure 9).

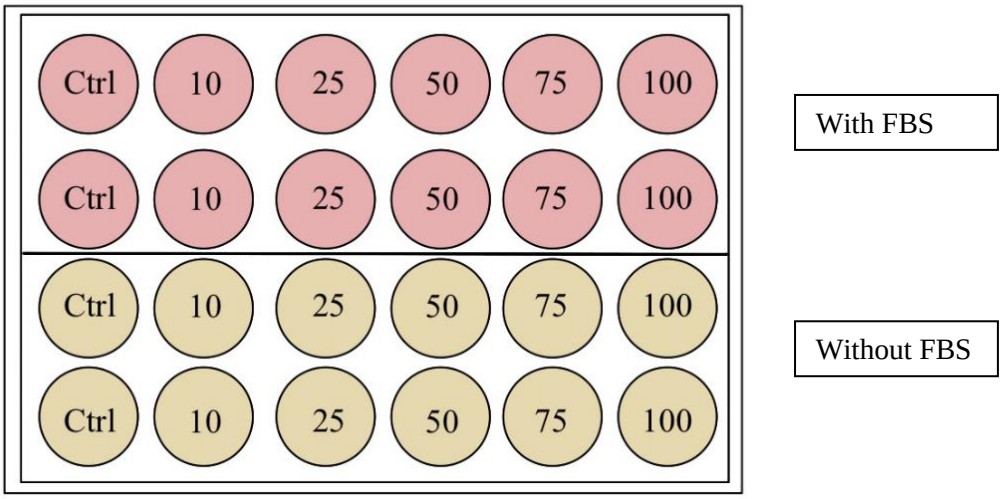

Figure 9: Layout of 24-well plate, cells were treated by duplicate with or without FBS and using different concentrations of PAA.

After 24h and 48h of treatment, the supernatant from each well was collected and kept at -20°C until further used and cell viability measured using two different methods.

1) Cell Counting Kit-8 (CCK-8)

CCK-8 assay is a highly sensitive, non-radioactive colorimetric detection method used to determine the number of viable cells in cell proliferation or cytotoxicity assays. CCK-8 serves as an indicator for redox reactions. This reagent can catalyse the reduction of the tetrazolium salt WST-8 to produce a highly water-soluble, yellow-coloured formazan dye in the presence of dehydrogenases within live cells. The amount of formazan dye generated

is directly proportional to the number of viable cells, meaning that the depth of colour is directly correlated with cell proliferation and inversely related to cytotoxicity. Optical density (OD) values are measured at a wavelength of 450 nm using a microplate reader, allowing for the indirect quantification of the number of viable cells[53].

Following the manufacturer recommendations, and following incubation with PAA, the media was removed. Each well was rinsed with PBS and then 10µL CCK-8 solution with 90µL media (DMEM without FBS without high glucose) were added to each well. The plate was placed in the incubator for one hour and afterwards the absorbance at 450nm was determined to measure cell viability.

To evaluate if PAA could interfere with the absorbance measurements, 50 µL of the supernatant from each well was transferred to a new plate and the absorbance measured using the CCK-8 assay and following the steps outlined above.

Trypan Blue Staining

The principle of Trypan Blue staining for distinguishing between live and dead cells is based on the fact that healthy live cells possess intact cell membranes that actively exclude Trypan Blue, preventing it from entering the cell. In contrast, cells that have lost their viability or have compromised cell membrane integrity exhibit increased permeability, allowing Trypan Blue to penetrate and stain them. Typically, the loss of cell membrane integrity is considered indicative of cell death. Live cells remain unstained by Trypan Blue, while dead cells are stained with a pale blue colour. Following Trypan Blue staining, cell viability can be quantitatively assessed with a high degree of precision either through direct counting under a microscope or by capturing microscopic images followed by counting[54].

Following 24h of incubation with PAA, the media was removed and 500 µL media (DMEM high glucose without FBS) was used for removing any remaining PAA. Then 100uL of Trypsin was added to each well for 2-3mins and neutralized with 1mL of media (DMEM high glucose with 10% FBS), and collected into individual Eppendorf tubes for analysis of cell viability. For this purpose, 10µL from each Eppendorf and 90µL of Trypan Blue staining solution were mixed and dropped onto cells counting slides, and cell viability was measured using a LUNA-II™ Automated Cell Counter (Logos Biosystems)

3.6. Magneto-mechanical treatments

A 3D printed and assembled device built by the team of Professor Angelakeris at the University of Thessaloniki in Greece, was kindly provided to be used for these experiments. The device incorporates two opposing neodymium iron boron (Nd-Fe-B) permanent magnets on a disk, driven by a direct current motor with a maximum voltage of 12V. It was determined that under a 12V voltage supply, the rotating disk can generate an alternating magnetic field with a frequency of 10Hz and a magnetic flux density of 160mT. The cross girder is designed to hold the sample dishes to be tested at two designated positions along the black dashed lines (Figure 10).

The main purpose of this experiment was to assess the impact of the magnetic field on the murine macrophages in the presence and absence of PAA.

For carrying out these sets of experiments, 150,000 RAW 246.7 were seeded into Petri dishes with a diameter of 3.5 cm, containing 2 mL of culture medium (high glucose DMEM with 10% FBS). After 24h the media was replaced by 1.5 mL of fresh media (high glucose DMEM with 0.5% FBS) for another 24 hours. Subsequently, the cells were exposed to 75 μg/mL of PAA suspended in 10% FBS, 0.5% FBS or and serum-free media (Figure 11).

In order to investigate the potential effects of the magnetic field on untreated cells, Petri dishes were prepared as well for each treatment condition. One set of dishes was exposed to the magnetic field, while the other set was placed at room temperature for the duration of the treatment serving as a control.

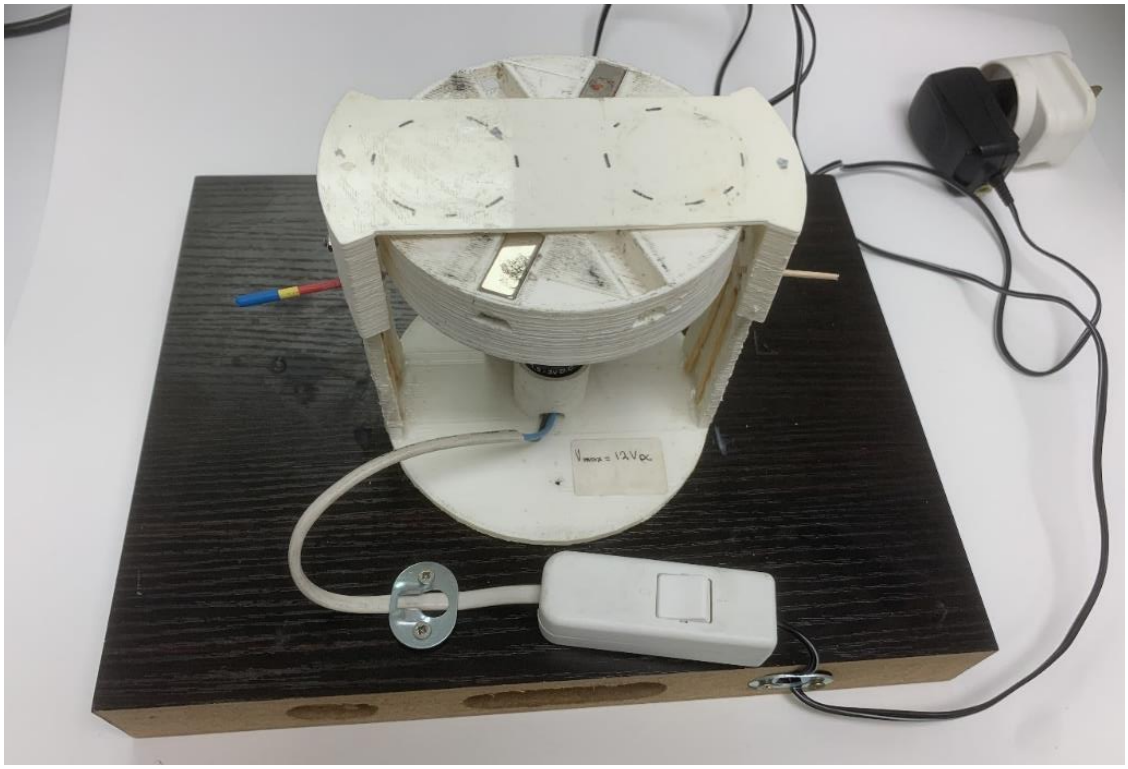

Figure 10: Photo of the apparatus for magneto-mechanical treatments. The device was built and kindly provided by the team of Professor Angelakeris at the University of Thessaloniki, Greece.

Table 11: Layout of the experimental procedure for the application of the magnetic field. In thi9s case Petri dishes seeded with 150,000 cells were used.

	no FBS	0.5% FBS	10% FBS
with NPs			
without NPs			

Exposure to the alternating magnetic field:

Petri dishes were first subjected to 30-minute treatment on the alternating magnetic field device and then returned to the incubator for 2 hours (this was considered one treatment cycle) and repeated once. Simultaneously, a control group with the same culture medium was kept at room temperature as a blank control during the magnetic field treatment.

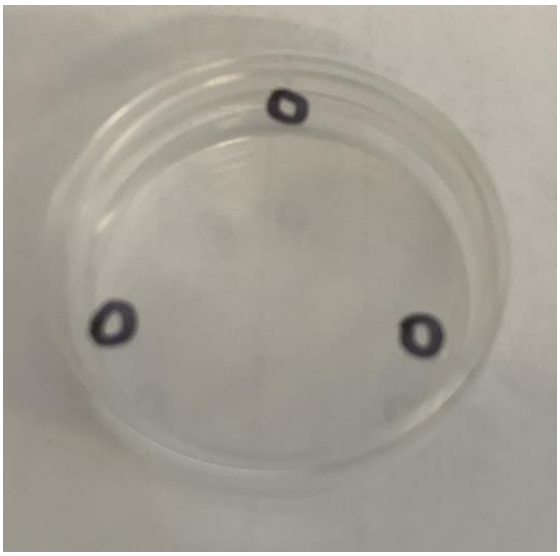

Figure 12: Photo of the marks in the Petri dish. Pictures were taken with a microscope before magnetic field treatment, and the photographed area was marked.

Before exposing the cells to the magnetic field treatment, three circles were drawn on the surface of each of the Petri dishes and images captured with an optical microscope (BRAND) (Figure 12). After both magnetic field treatments, micrographs were immediately taken again at the same locations to avoid bias. Subsequently, the dishes were returned for 24 hours of incubation and microscope images taken once again. Then, cell viability was assessed using the trypan blue staining method.

The supernatant from each dish was collected and kept at -20°C until further.

3.8. Transmission Electron Microscopy

Transmission Electron Microscopy (TEM) allows the visualization of submicron-scale structures (smaller than 0.2 μm), which are not discernible under optical microscopy. TEM was used to determine whether PAA particles were internalised and the effect that they could exert of the RAW 246.7 cells after magnetic field treatment.

First, cells were cultured on glass slides (placed inside the Petri dish) following the same procedure described in the previous section (magneto mechanical treatment). After the

completion of the magnetic field treatment, the fixative solution (2.5% glutaraldehyde) at 37°C was added to the Petri dish, incubated at room temperature for 1 hour and then storage at +4°C until further processing by Tiina O'Neil (Conway Institute, University College Dublin). TEM images were obtained using an FEI CM20 microscope operating at 200 kV, equipped with a Gatan GIF 200 energy filter for EF-TEM elemental mapping.

3.9. Gelatine Zymography

Following the magnetic field treatment, the media from each experimental group was promptly collected, subjected to centrifugation at 13,000 rpm for 5 minutes to eliminate any debris, and the resulting supernatant was stored at -20°C until further utilization.

To quantify the total protein concentration in the 'post-treatment' media and the volume to be loaded per sample, the Bradford method was employed. This assay relies on a dye-binding technique, wherein distinct colour changes of the dye correspond to varying protein concentrations. Initially, a series of dilutions containing known concentrations of bovine serum albumin (BSA), ranging from 0 μg/mL to 400 μg/mL, was prepared. Standard curves were constructed, and linear regression analysis was employed to calculate the protein concentration in the samples.

After uniform protein concentrations of each experimental group. Gelatin zymography was used to detect the activity of MMP-2 and MMP-9. Samples were subjected to 10% SDS-polyacrylamide gel electrophoresis with copolymerized gelatin (0.2%) incorporated as a substrate for gelatinolytic proteases. Electrophoresis was conducted in a buffer solution (250 mM glycine, 25 mM Tris-HCl at pH 8.3, and 0.1% SDS) at 150V for a duration of 2 hours. Following electrophoresis, the gels underwent a series of washes: three times with 2.5% Triton X-100 for approximately 20 minutes each, followed by two washes with zymography buffer for about 20 minutes each. Subsequently, the gels were placed in a water bath and incubated at 37°C for 7 days. RAW 246.7 cells were treated with LPS (LPS would induce RAW 246.7 cells polarization toward M1, thus containing high amounts of MMP-2 and MMP-9), was used as control.

To visualize gelatinolytic activity, the gels were stained using a staining solution (40% methanol, 10% acetic acid, and 0.1% (w/v) Coomassie Blue R-250) for 1 hour, followed by a 1-hour distaining process in 4% methanol with 8% acetic acid. MMP-2 and MMP-9 were identified by its mol. wt. when compared with RAW 246.7 cells were treated with LPS. Gel images were captured using the ChemiDoc XRS System (Bio-Rad, Hercules, CA), and the intensity of the bands was quantified using Biorad Image Lab 6.1 software. The gelatinolytic activity of each band was expressed as arbitrary units of density per milligram of protein [55].

3.10. Statistical analysis

Statistical analyses were carried out using Graph Pad Prism 9.0 software (San Diego, CA, USA). All results are shown as mean ± standard derivation (SD) from at least three independent experiments. Statistical significance differences between groups were calculated aplying One-way ANOVA and followed by Tukey or Dunnett multiple post-tests when appropriated. P-values less than 0.05 ($p<0.05$) were considered significant.

4. Results

4.1. Characterisation of MNPs

The PAA were chosen for carrying out this project on macrophages. The prolonged storage of those MNPs resulted in a tendency to aggregate. Therefore, as a pre-experimental step, the dispersion was always sonicated for 30 minutes prior to any experimental procedure even thought they had been filtered (0.22µm) to warrant the sterility of the samples (Figure 13).

The negatively charged PAA were further characterized under different conditions using different diluents. PAA at a concentration of 100 µg/ml (concentration to be used for further experiments), exhibited the most uniform and stable distribution in PBS. However, in water and DMEM, whether containing FBS or not, they tend to aggregate (Figure 14).

The size and zeta potential of the MNPs were measured and analysed using the Malvern Zetasizer software in triplicate. DMSA-MNPs exhibited the worse stability while AEPA-MNPs and PAA exhibited a better stability, although some aggregates were also present (Figure 15).

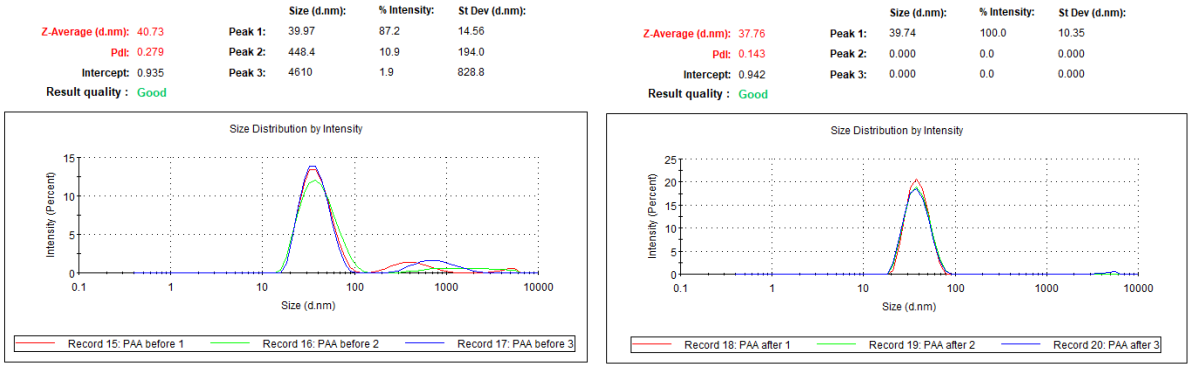

(A) (B)

Figure 13: PAA were used at a concentration of 100 µg/ml. The MNPs size and dispersion were assessed in water following 30 minutes of sonication. The measurements were conducted before (A) and after filtration (B)

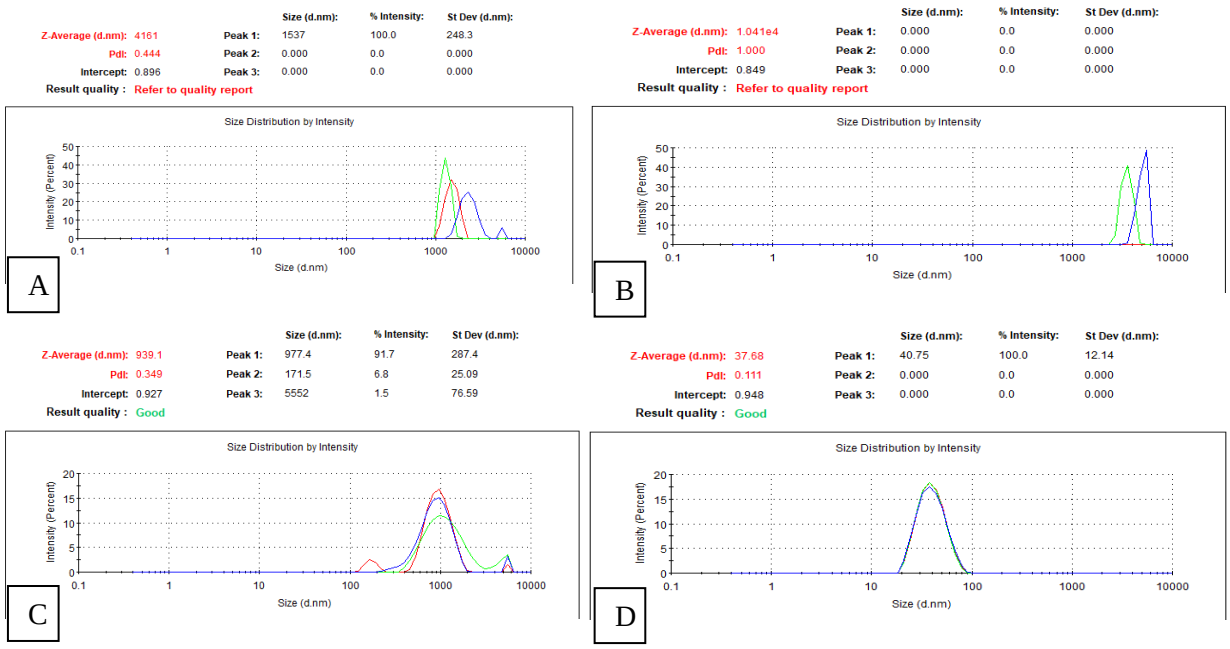

Figure 14: PAA size was measured at a concentration of 100 µg/ml following 30 minutes of sonication. Different media were employed, including DMEM with 10% FBS (A), DMEM without FBS (B), water (C), and PBS (D).

Figure 15: The size of the three developed MNPs in water were tested at a concentration of 300 µg/ml, following 30 minutes sonication and filtration. The MNPs included PAA (A), DMSA-MNPs (B), and AEPA-MNPs (C).

4.2. Blood compatibility tests

These experiments were performed in order to investigate the potential interaction of the MNPs with RBCs (haemolysis tests) and with platelets.

4.2.1. Haemolysis Test

Tests were performed in duplicate for the three types of nanoparticles and with blood from at least three different donors, with and without 0.5% PPP. The absorbance of the supernatant after incubating RBCs with the MNPs was measured at 540 nm. RBCs treated

with Triton were used as the positive control and set as 100% haemolysis for quantification, while RBCs without any treatment served as the negative control. For PAA, in the presence of 0.5% PPP, significant differences were observed only at concentrations of 75 and 100 µg/mL, while in the absence of PPP, all concentrations showed toxicity. For DMSA-MNPs, in the presence of 0.5% PPP, a significant effect was observed only at a concentration of 50 µg/mL, while in the absence of PPP, there were no significant differences at any of the concentrations tested. In the case of AEPA-MNPs, no significant differences were found at any concentration, regardless of the presence or absence of PPP. (Figure 16).

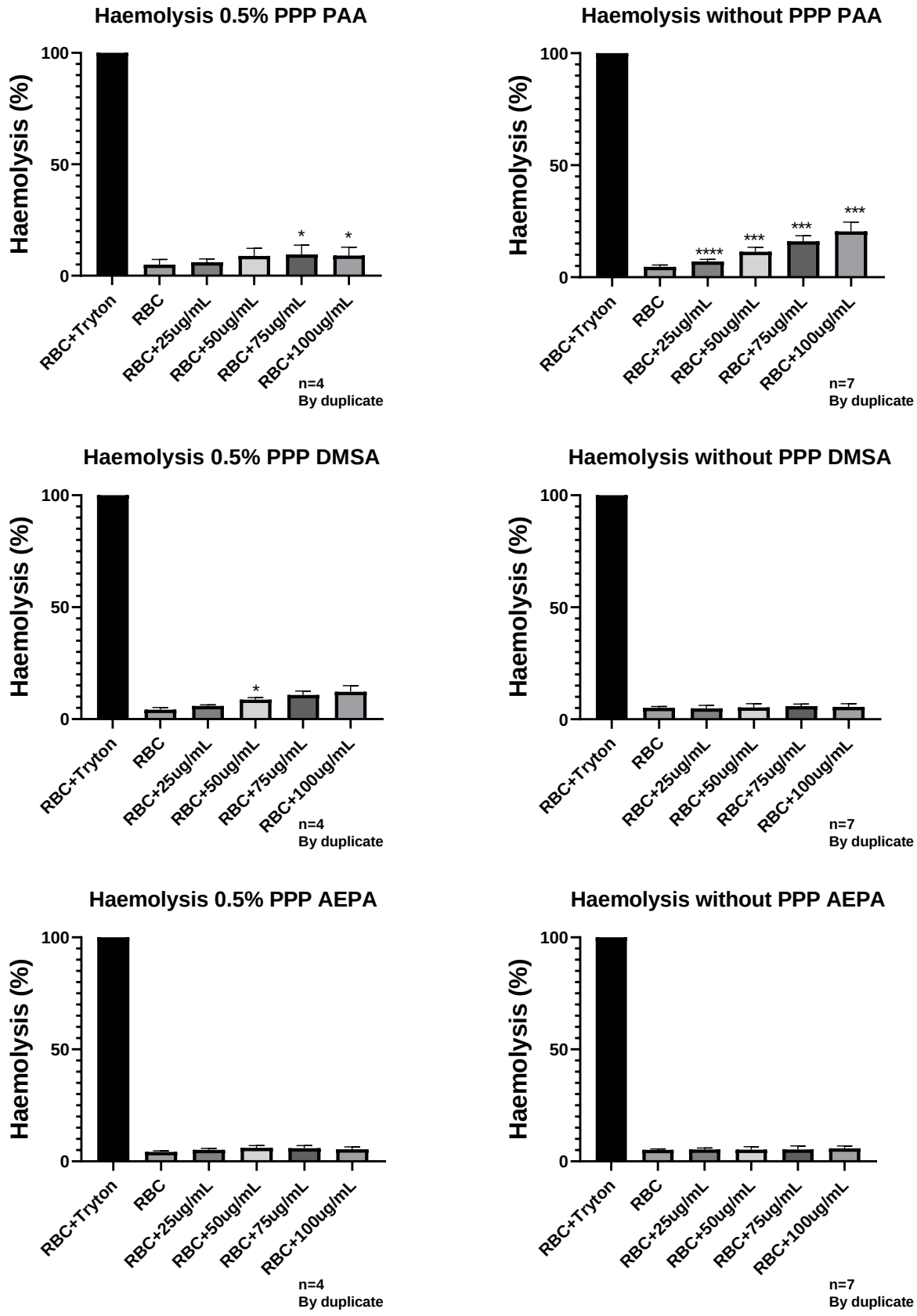

Figure 16: Statistical analysis of the haemolysis test for the three MNPs (PAA, DMSA-MNPs and AEPA-MNPs) at different concentrations with and without 0.5% PPP. One-way ANOVA and Dunnett test post-test, * $p<0.05$; ** $p<0.01$; *** $p<0.001$; **** $p<0.0001$ vs RBC)

The RBCs exposed to different concentrations of NPs, were also prepared on slides using a Cytospin 4 and then visualized under a microscope at 50X magnification. On the naked eye, for PAA, some ruptured RBCs were observed as the concentration increased. However, there was no significant difference in RBCs for DMSA-MNPs and AEPA-MNPs (Figure 17). The results are consistent with those in Figure 16.

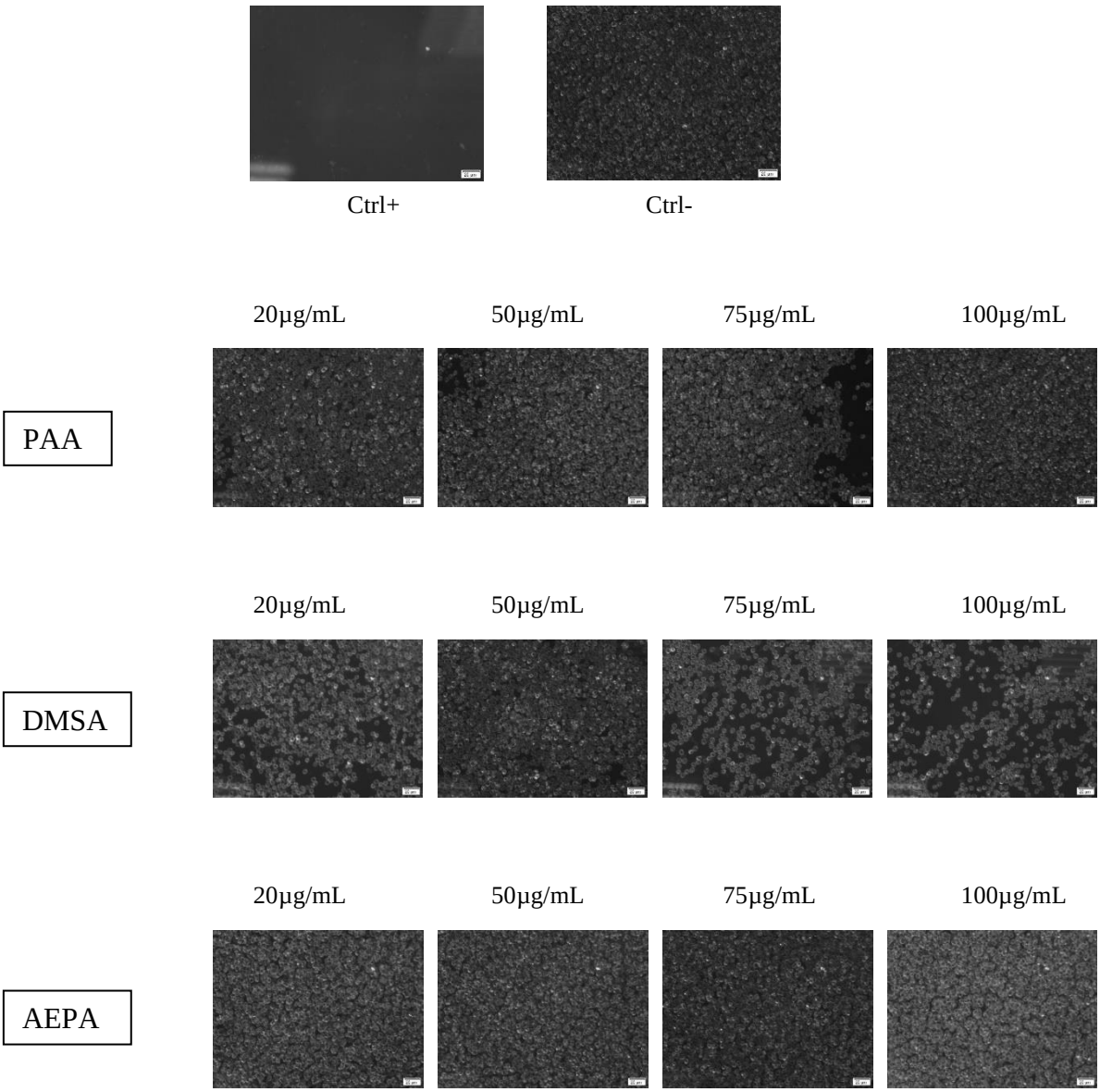

Figure 17: Images of the RBCs after incubation with different concentration (25, 50, 75 and100 µg/mL) of MNPs in the presence of PPP. 50X magnification. RBCs with Triton were used as the positive control (Ctrl +), RBCs without any treatment served as the negative control (Ctrl +).

4.2.2. Light transmission aggregometry

PRP containing varying concentrations of the three MNPs were kept under stirring for 30 minutes to investigate if the MNPs were able to induce platelet aggregation. PRP stimulated with collagen was considered as the 100% positive control, and PRP subjected to stirring alone served as the negative control. Any of the MNPs tested induced platelet aggregation (Figure 18). There was no significant difference in the platelet count observed under the microscope (Figure 19).

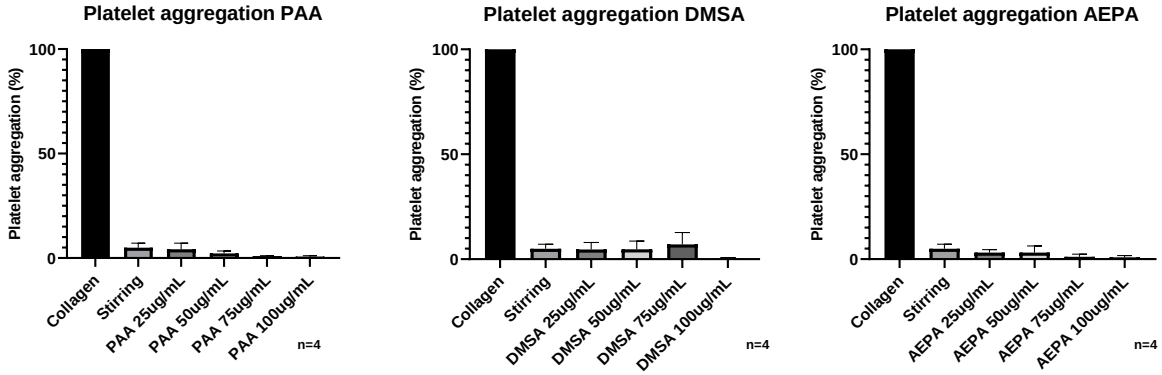

Figure 18: Statistical analysis from the light transmission aggregometry of three NPs (PAA, DMSA_MNPs and AEPA-MNPs) at different concentrations (One-way ANOVA and Dunnett test post-test, * $p<0.05$; ** $p<0.01$; *** $p<0.001$; **** $p<0.0001$ vs Stirring).

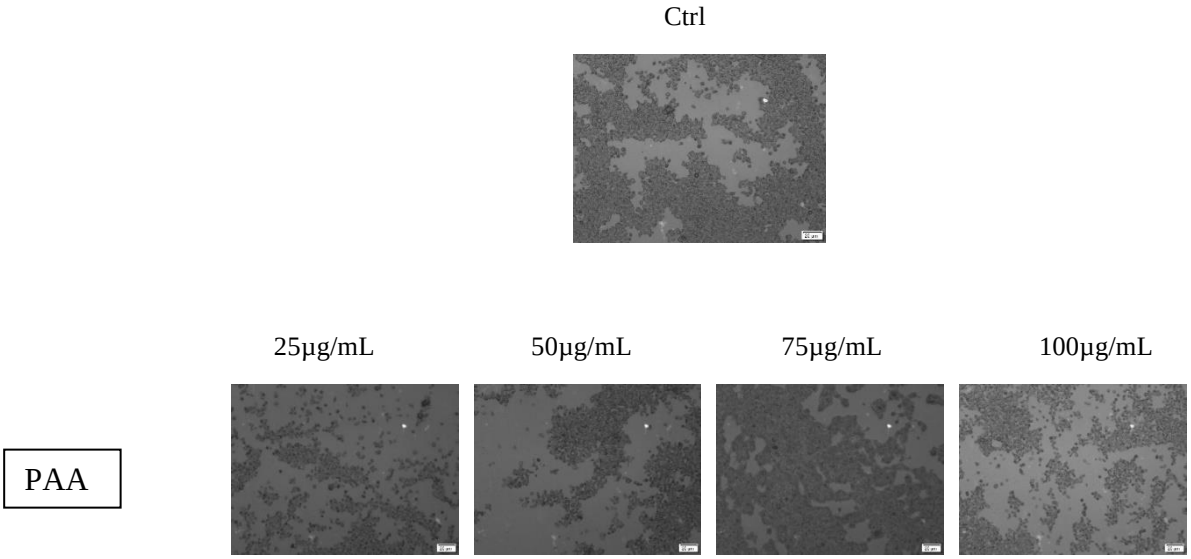

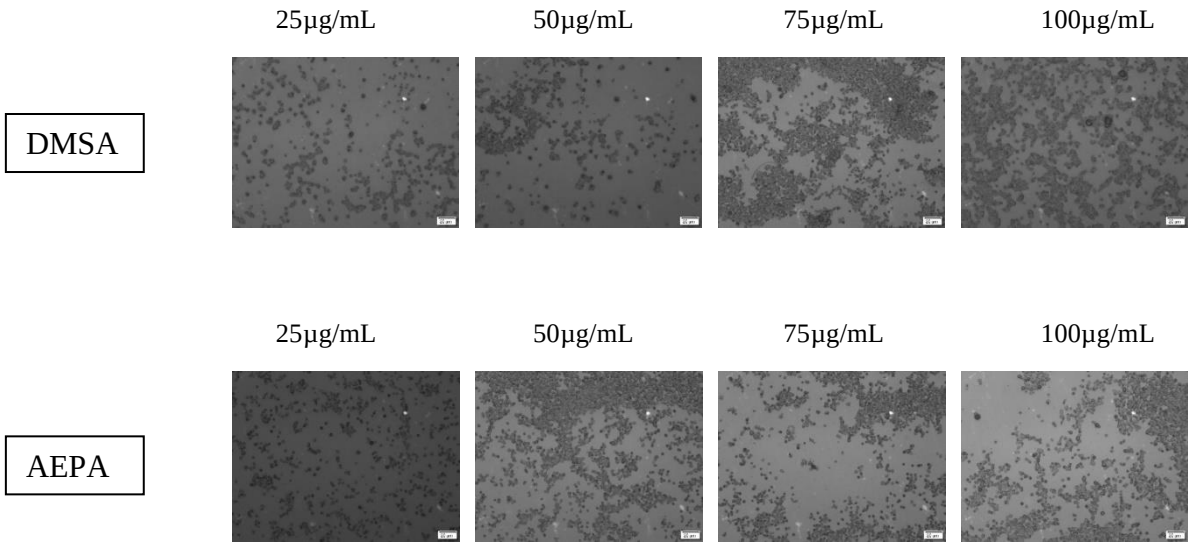

Figure 19: Images of the PRP with different concentration (25, 50, 75 and100 µg/mL) of MNPs. PRP without any treatment served as the control.

4.3. Cell viability

The cell viability of macrophages (RAW 246.7) incubated with different concentrations of PAA for 24h and 48h was first tested. The viability of the cells in the absence of MNPs was set as 100% of viability and used as control. Due to the interference of the MNPs with the absorbance when using the CCK-8, results obtained were not reliable and trypan blue was used instead for analysing cell viability after exposure to the PAA.

The results indicated that different concentrations of PAA and FBS have varying effects on RAW 246.7 cells. When using 0% FBS medium, significant differences were observed at concentrations of 25, 50, 75 and 100 µg/mL after 24 and 48h incubation. For 0.5% FBS media, significant differences were observed at concentrations of 25, 50 and 75 µg/mL after 24h, while after 48h, significant differences were observed at concentrations of 25, 50, 75 and 100 µg/mL. In the case of 10% FBS medium, significant differences were observed only at concentrations of 100 µg/mL after 24h, while after 48h, there were no significant differences at any of the concentrations tested (Figure 20).

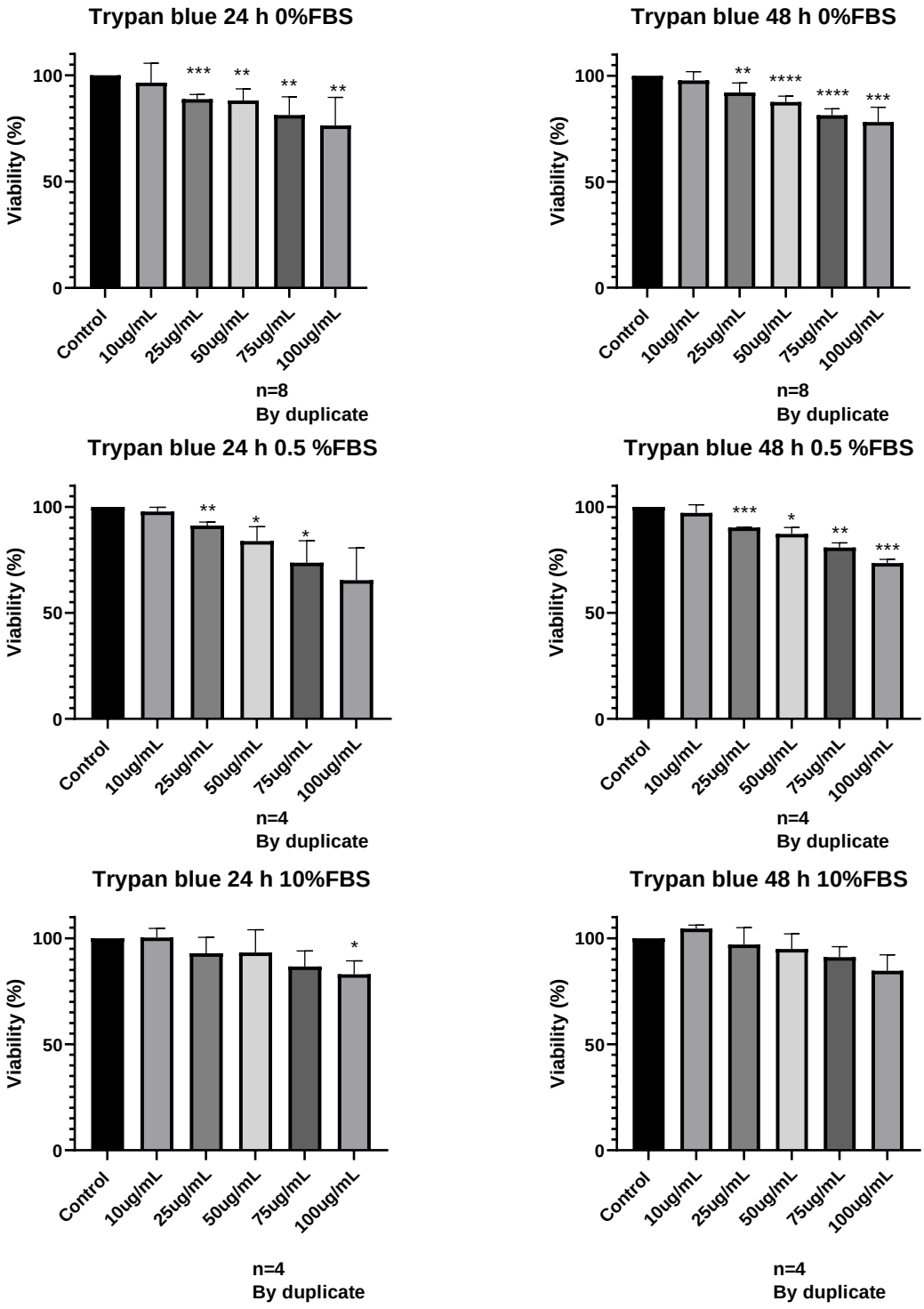

Figure 20: Statistical analysis of cell viability of PAA different concentration of FBS (0%, 0.5% and 10%) in media. Raw 264.7 cell viability was measured at 24 and 48 hours. One-way ANOVA and Dunnett test, * $p<0.05$; ** $p<0.01$; *** $p<0.001$; **** $p<0.0001$ VS control.

4.4. Magneto-mechanical treatments

Based on the viability results from the previous section, 75ug/mL of PAA was chosen as the concentration to be tested for the magneto-mechanical treatments. As stated in section 3.6, cells were first exposed to the alternating magnetic field device for 30-minute, returned to the incubator for 2 hours, and were again exposed to the alternating magnetic field device for 30-minute, and finally returned to the incubator for 2 hours. This process was regarded as magneto-mechanical treatments. Cells in the same medium were not exposed to alternating magnetic field device at room temperature as controls.

Cells (those exposed to the alternating magnetic field device and those kept at room temperature as control) were visualised (on the marked places in the Petri dishes for avoiding bias) using an optical microscope (50X magnification) at the following three time points: before the treatment (time 0), end of the treatment (time 1) and returned to the incubator for 24h after the treatment (time 2) (Figure 21).

For the statistical analysis, cells exposed to the magneto-mechanical treatment but not incubated with PAA were used as control and their viability measured with trypan blue set as 100%.. The cell viability test used (trypan blue) confirmed that the concentration of 75 µg/mL PAA only exhibits an impact on the activity of RAW 264.7 cells after magnetic field treatment (Figure 22).

A B C D

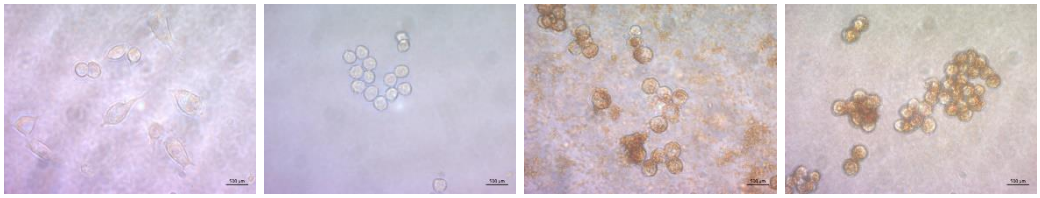

Before the treatment (time 0)

Cells exposed to alternating magnetic field device

A_1 B_1 C_1 D_1

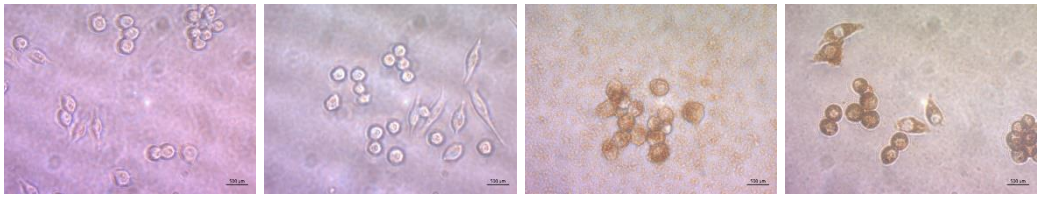

Cells not exposed to alternating magnetic field device (control)

A_2 B_2 C_2 D_2

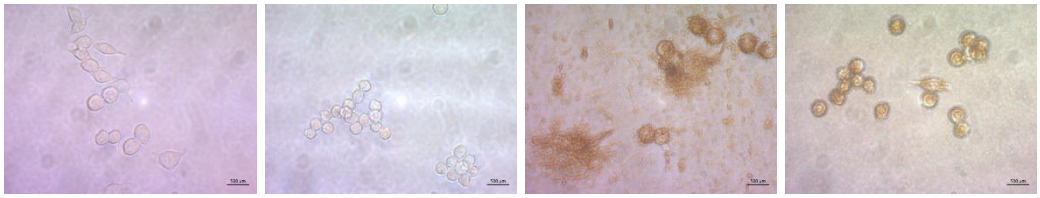

End of the treatment (time 1)

Cells exposed to alternating magnetic field device

A_1 B_1 C_1 D_1

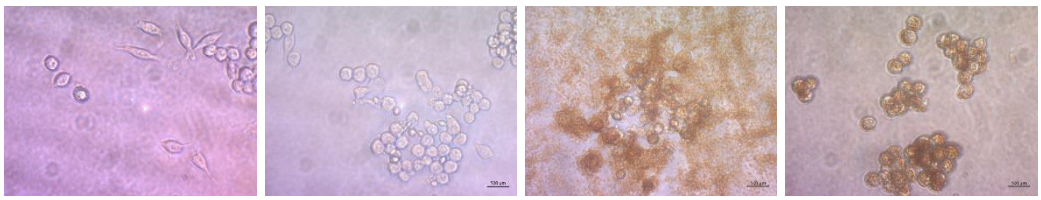

Cells not exposed to alternating magnetic field device (control)

A_2 B_2 C_2 D_2

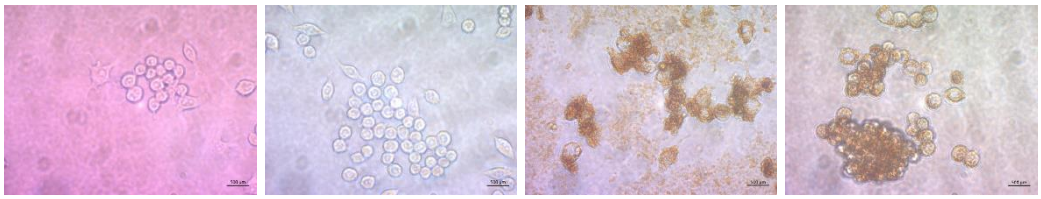

24h after the treatment (time 2)

Figure 21: Images of the RAW 246.7 cells under optical microscope at 50X magnification. A) Cells in free FBS media without PAA; B) Cells in 0.5% FBS media without PAA; C) Cells in free FBS media + 75 µg/mL PAA; D) Cells in 0.5% FBS media + 75 µg/mL PAA. 1) Cells exposed to the alternating magnetic field device.2) Cells in the same medium were not exposed to alternating magnetic field device at room temperature as controls.

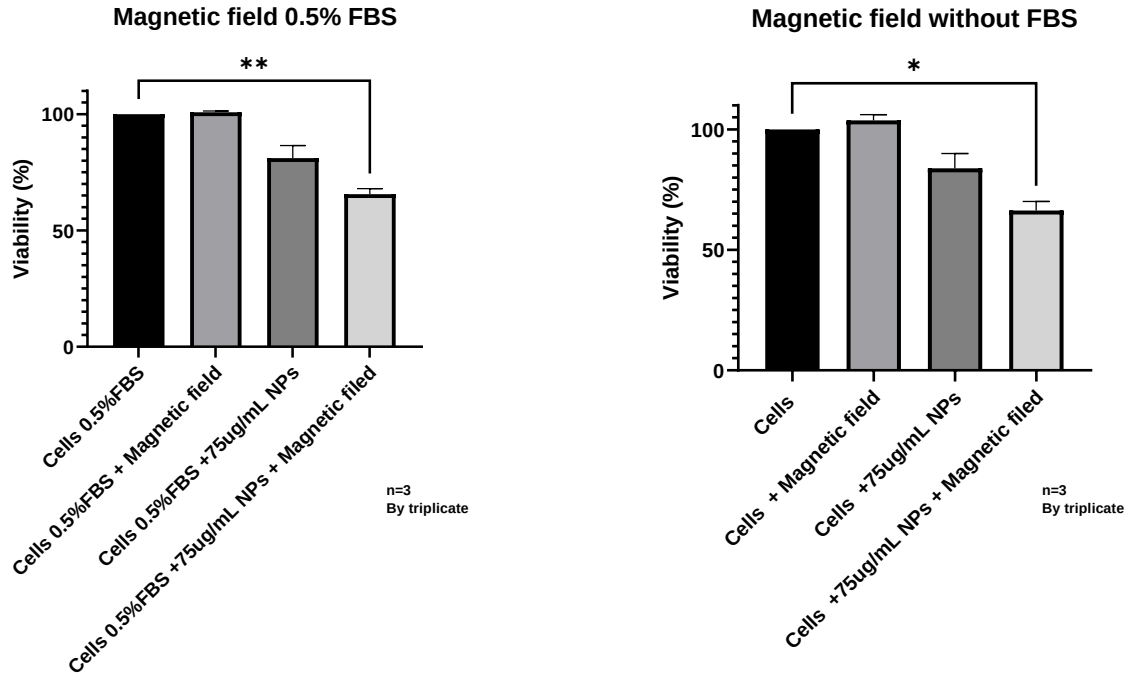

Figure 22: Graphical representation of the results obtained from the viability of RAW 246.7 cells incubated with and without PAA in A) 0.5% FBS media and b) free FBS media. One-way ANOVA and Tukey post-test, * $p<0.05$; ** $p<0.01$; *** $p<0.001$; **** $p<0.0001$ VS control.

4.5. Transmission electron microscopy

To confirm whether PAA enter RAW 246.7 cells and exerted any ultrastructural damage on the cells, transmission electron microscopy (TEM) was employed. A small amount of PAA were distributed outside the cell membrane, closely adjacent to the cells and clusters were found inside the cells.

In the control group without magnetic field treatment, it can be observed that MNPs aggregate around the cell membrane, with a significant portion being engulfed to form vesicles that accumulate within the cell. Moreover, there is a continuous formation of secondary lysosomes through the fusion of primary lysosomes with these vesicles.

Following magnetic field treatment, cells in the 0%FBS and 0.5%FBS groups exhibit a state of lysed cell death, while in the 10%FBS group, MNPs did not enter the cells in large quantities, possibly due to the effect of high FBS concentrations that may have reduced the internalisation of MNPs.

Without magnetic field treatment:

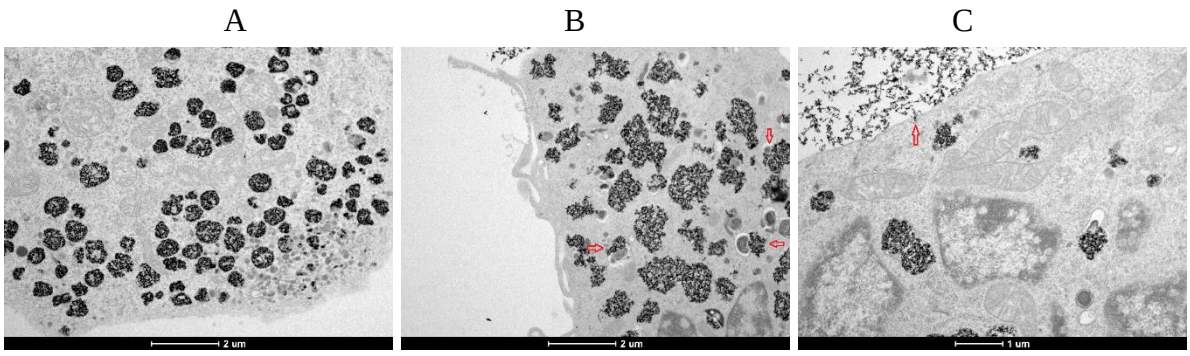

With magnetic field treatment:

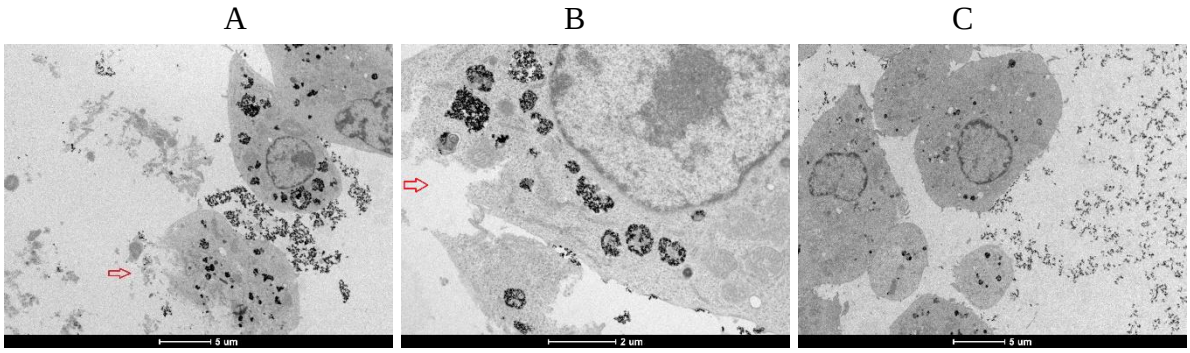

Figure 23: Images of the RAW 246.7 cells exposed to PAA after magnetic field treatment; A) Cells incubated in free serum media; B) Cells incubated in 0.5% FBS media; C) Cells incubated in 10% FBS media. It can be observed that a significant amount of PAA is present inside the cells.

4.6. Gelatine zymography

After magnetic field treatment, cell culture supernatant was collected for protein quantification with the aim of looking at gelatinase activity by gelatine zymography RAW 246.7 cells treated with LPS was used to identify MMP-2 and MMP-9 in the gel, the intensity of the bands obtained taken as 100% and use to normalise the data for analysis.

During obesity-related inflammation, the levels of MMPs increase could be due to the proliferation of M1 macrophages. Experimental results indicate that there is a significant difference in the levels of both MMPs after magnetic field treatment.

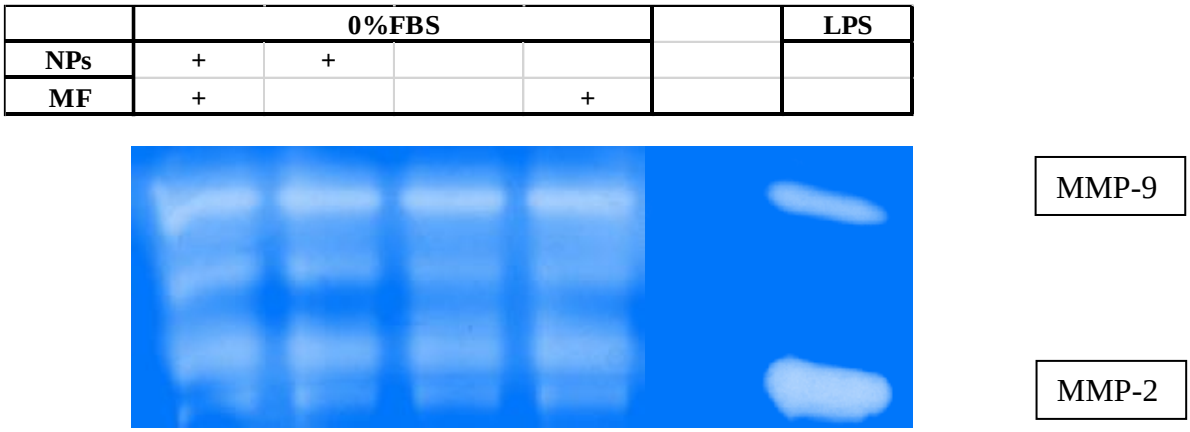

Figure 24: Representative gelatine zymography. RAW 246.7 cells treated with lipopolysaccharide (LPS) were used as a 100% control.

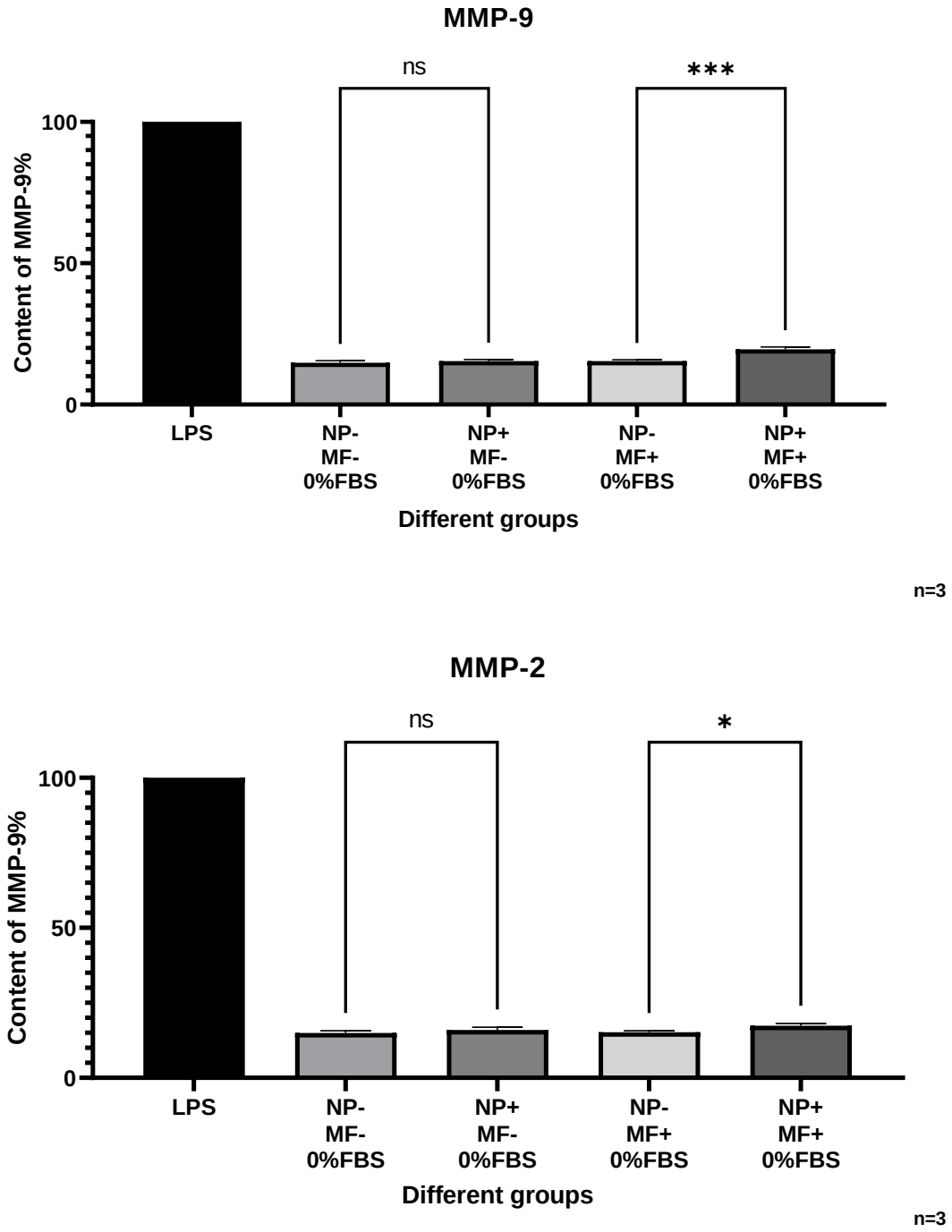

Figure 25: Statistical analysis of the results obtained from the impact of the presence of PAA-MNP, and exposure to magnetic field treatment on RAW 264.7 cells on MMP-2 and MMP-9. In the one-way ANOVA (Tukey test, * $p<0.05$ VS control; ** $p<0.01$ VS control; *** $p<0.001$ VS control; **** $p<0.0001$ VS control) analysis depicted in the figure, each group was compared to the group cells only.

5. Discussion

5.1. Properties and toxicity of MNPs

With the advancement of synthetic techniques, a series of shape-controllable, stable, and monodisperse MNPs have been successfully prepared. Their magnetism facilitates facile aggregation, separation, directed motion, and positioning. Prior to their actual clinical application, it is imperative to conduct toxicological studies on these MNPs.

In this experiment, the particle sizes of three types of MNPs employed (PAA, DMSA, AEPA) were initially determined. Some evidence suggests that MNPs larger than 200 nm can reach the liver and spleen through mechanical filtration, and the accumulated MNPs in these organs may induce oxidative stress, inhibiting the action of antioxidants and consequently causing damage to the organs[56]. However, smaller is not always better for MNPs. MNPs with sizes smaller than 10 nm, for instance, can be captured by the kidneys, also leading to the induction of oxidative stress. There is evidence indicating that these small MNPs may also breach the blood-brain barrier, accumulate in the brain, and cause irreversible harm[40]. Therefore, MNPs within the size range of 10-100 nm are considered the preferred dimensions for in vivo applications[57]. According to the DLS test results in Section 4.1, the particle sizes of the three MNPs (PAA, DMSA, and AEPA) are approximately 45 nm, 33 nm, and 28 nm, respectively, all falling within the preferred range. Due to the high saturation magnetization of these three MNPs, they can generate strong magnetic forces even in small sizes, enabling them to operate in more intense magnetic field environments. This characteristic allows for enhanced targeting precision and faster response to magnetic fields[62]. The results from Figure 13 in the DLS analysis indicate that approximately 10% of PAA underwent aggregation before filtration. Despite all three MNPs possessing superparamagnetic structures at room temperature, meaning they exhibit magnetism in the presence of an external magnetic field and lose it when the field is removed, the pre-treatment of MNPs involves a 30-minute ultrasonication step before each magnetic field therapy session. This step ensures uniform distribution of MNPs in the solvent prior to magnetic field exposure.

The DLS experiments also assessed the distribution of PAA in various solvents, revealing significant differences. Apart from the mentioned spontaneous aggregation, a more likely reason for this disparity is the variation in the particle size of MNPs in different dispersing media. Research indicates that introducing 40 nm copper into deionized water and RPMI-1640 medium resulted in a volume increase of 28 times, whereas the increase was only 9 times compared to placing it in serum-containing medium [58]. The variation in the particle size of MNPs directly influences the cellular uptake during subsequent treatment processes. Therefore, selecting an appropriate surface coating for MNPs is crucial for their stability. The three MNPs used in the experiment exhibit optimal anisotropy constants (K), achieved by altering their shapes to obtain the best anisotropy constants. This implies the formation of numerous dangling bonds around the surface atoms of MNPs, rendering them unsaturated and more prone to forming stable structures through bonding with other atoms. Consequently, they demonstrate higher chemical reactivity[59]. Three types of NPs with different surface coatings: PAA, DMSA, and AEPA were developed for this project. According to the DLS measurements, all three types of MNPs exhibited small average diameters and stable dispersion in water and PBS, which are ideal characteristics for therapeutic purposes.

Different surface coatings not only impact the particle size of MNPs but also influence their biocompatibility. This project focused on experimental research into the blood compatibility of MNPs. Mature RBCs, lacking a cell nucleus and organelles, have limited self-repair capabilities after damage. The direct interaction between MNPs and RBCs can damage their cell membranes, leading to membrane rupture or hemolysis[60]. In experiment 4.2.1, it was observed that PAA indeed caused death in RBCs; however, after the addition of 0.5% PPP, the damage to RBCs was significantly reduced. Due to the current inability to thoroughly analyze serum components, the mechanism by which PPP reduces RBC damage remains unclear. Investigating the potential interactions of MNPs with platelets is also a significant aspect of blood compatibility testing. Platelets, disc-shaped blood cells, undergo structural changes and adhere to the vessel wall to form a clot when the vascular wall is damaged, playing a crucial role in hemostasis[61]. When foreign bodies such as MNPs enter the bloodstream, it is essential to investigate whether they induce platelet aggregation, leading to the formation of clots that may obstruct blood

vessels. Initially, based on the zeta potential measurements of MNPs in DLS, PAA and DMSA were found to be negatively charged, while AEPA was positively charged. The surface of platelets, however, carries a negative charge[62]. This could potentially lead to aggregation between AEPA and platelets, but experimental results from section 4.2.2 demonstrated that none of the three MNPs exhibited potential mutual interactions with platelets. In fact, the zeta potential itself reflects the stability of MNPs in a medium, and typically, MNPs with an absolute zeta potential value in the range of 20-30 mV remain stable in suspension, as surface charges help prevent particle aggregation[63].

The reason for using PAA instead of the other two in this experiment is that PAA, as one of the latest MNPs, exhibits significantly improved stability. Some other studies indicate that PAA does not undergo self-degradation even after prolonged use, posing minimal ecological toxicity. Moreover, PAA has the largest particle size among the three, resulting in greater forces and torque generated in the magnetic field, making it more effective in producing the NMMA effect[64]. Therefore, as a novel MNPs coating, PAA holds promising prospects for development.

Before applying magnetic field therapy using PAA, it is necessary to assess the cytotoxicity of PAA. Some studies suggest that the cytotoxicity of MNPs tends to increase with higher concentrations[65]. Consistent with the conclusions drawn in Section 4.3 of this experiment, cytotoxicity was concurrently assessed under three different conditions: no addition of FBS, addition of 0.5% FBS, and addition of 10% FBS. Results showed similarities between the groups without FBS and with 0.5% FBS serum starvation treatment. Serum starvation treatment enhances cellular uptake of MNP drugs, potentially improving the overall therapeutic effect. The inclusion of 10% FBS aimed to simulate the in vivo biological environment[66].

The choice of using 75 μg/mL of PAA in experiment 4.4 was based on a comprehensive consideration of the results obtained in experiment 4.3. However, a challenge was encountered during the experiment regarding the inability to accurately detect CCK-8. CCK-8 can reduce dehydrogenases in the mitochondria of cells to produce a highly water-soluble yellow formazan product. The quantity of the generated formazan is proportional to the number of viable cells, and by measuring its absorbance, the number of viable cells can be indirectly reflected[67]. However, during the experiment, it was observed that when

measuring absorbance, it was not possible to completely eliminate the influence of PAA, suggesting that PAA itself might absorb a portion of light, leading to inaccurate results. Consequently, the final approach involved cell counting using Trypan Blue staining. Trypan Blue stain, serving as a cell viability dye, was employed to assess the integrity of cell membranes and determine cell viability. Living cells remain unstained, while dead cells are stained light blue. Subsequently, cell counting was conducted using a cell counting chamber[54].

The primary determinant of the cytotoxicity of MNPs is their ability to interact with cells, typically occurring after the internalization of MNPs by cellular uptake, with endocytosis being the primary pathway for MNP uptake by cells. At this stage, the surface coating of MNPs plays a crucial role, enhancing biocompatibility and altering the permeability of the cell membrane to facilitate the entry of MNPs into cells, achieving the desired effects. TEM results indicate that, following magnetic field treatment, although a portion of PAA is adsorbed on the cell membrane surface, a substantial amount of PAA is already present within the cells[56]. After the cellular uptake of MNPs, the toxicity may arise from the dissolution of the surface coating, leading to the release of toxic heavy metal ions from the core. It has been confirmed that most internal metals or metal oxides in MNPs can induce harm such as oxidative stress, DNA damage, or enzyme inactivation[68]. Typically, following cellular uptake, MNPs are enclosed within lysosomes and undergo dissolution. In experiment 4.5, TEM observations revealed that MNPs can indeed be observed within lysosomes after cellular uptake. The acidic pH (pH 5.5) inside lysosomes facilitates the dissolution of their surface coating, releasing potentially toxic heavy metal ions[69].

In conclusion, the prevailing fact with most MNPs today is that the internal metals or metal oxides are highly toxic. Therefore, for further toxicological studies on MNPs, it may be worthwhile to focus on functionalization and stabilization of the surface coating, aiming to selectively alter their properties. Alternatively, efforts could continue in developing magnetic metal compounds that are inherently low or non-toxic. Another obstacle complicating the toxicity assessment of MNPs is the potential toxicity when used in conjunction with other therapeutic drugs or materials, an aspect that has not received significant attention.

5.2. Principles of Treatment

ATMs in the context of obesity, tend to polarise towards the M1 phenotype, triggering inflammation. However, the functional status of macrophages is more complex[70] . Studies indicate that during obesity, both M1 and M2 polarizations increase. For instance, in obese tissues, hypoxia is a significant characteristic. Under hypoxic conditions, cells produce lactate through glycolysis, recruiting a large number of macrophages. This activates G protein-coupled receptors on macrophages, promoting their polarization towards the M2 phenotype[70].

Macrophages also play an indispensable role in lipid metabolism. M1 macrophages synthesize lipids and produce inflammatory lipid mediators such as leukotrienes, while M2 macrophages tend to take up and oxidize lipids. When obesity occurs, AT releases a large number of lipid-filled exosomes. The uptake of these lipids by ATMs, induces their polarization toward the M1 phenotype. These lipids play a crucial role in the membrane remodelling of M1 macrophages and the synthesis of inflammatory mediators. They actively regulate the inflammatory response of M1 macrophages and exacerbate inflammation[71]. Interestingly, at this point, ATMs do not necessarily polarise towards the M1 phenotype. Instead, a proportion of them polarise towards the M2, inhibit lysosomal biogenesis, impair lipid metabolism, increase lipid content in ATMs, and reduce overall lipid breakdown in ATMs[72]. Therefore, the chaotic polarization of ATMs is also a prominent feature of obesity.

In this experiment, the final results were quantified using the Coomassie Brilliant Blue staining method and gelatin zymography. The Coomassie Brilliant Blue staining method employed here was consistent with the one previously utilized in the toxicity assessment of MNPs. Gelatin zymography is a commonly employed protein analysis technique that accurately provides both protein mass and molecular weight analysis results. In this study, it was employed to assess the levels of two proteases, MMP-2 and MMP-9.

MMPs are a family of enzymes capable of degrading the extracellular matrix. MMP-2 is a

constitutive enzyme and MMP-9 is an inducible enzyme that plays an important role in inflammation, it is release by macrophages and its activity increase in AT[26]. MMP-2 and MMP-9 are the primary matrix metalloproteinases responsible for degrading collagen and gelatine in the basement membrane, and their activity can be assessed using gelatine zymography where acrylamide is copolymerised with gelatine and therefore degraded if MMP-2 and MMP-9 are present in the sample. From the Section 4.6, it can be deduced that a significant amount of both MMPs was indeed detected in RAW 246.7 cells after magnetic field therapy.

In this work we aimed to investigate the effect that PAA and the application of a LF-AMF could exert on macrophages. Although high concentrations of MNPs can potentially cause cell damage, this is not the intended outcome. Based on the cytotoxicity experiments it was determined that 75 µg/mL of PAA was found to be the highest concentration that did not cause direct harm to macrophages. There is evidence that LF-AMF, or the NMMA technology itself, can induce biophysical effects in living organisms, tissues, and cells. The prevailing hypothesis is that LF-AMF interacts with charged particles such as electrons within the biological system, leading to changes[73]. Due to the unclear nature of the physical mechanisms of this magnetic field effect, it is difficult to predict these changes. In addition, reports on this phenomenon often remain controversial and incomplete due to discrepancies in experimental conditions and replication of independent experiments[74].

However, by introducing MNPs into the LF-AMF system, the interaction between the LF-AMF and MNPs with diameters ranging from a few nanometres to several tens of nanometres can be thousands of times greater than that with individual electrons. This interaction allows the magnetic energy to become thermodynamically significant. This is the foundation for therapeutic methods using MNPs and offers advantages over pure magnetic therapy. The subsequent step involves converting the energy generated by the interaction between LF-AMF and MNPs into biochemical effects. For magnetic hyperthermia at frequencies f=100-800 kHz, this energy dissipates in the form of heat. In the case of NMMA, this energy is directly utilized as a localized force through magnetic manipulation, inducing deformation in biological molecules. These molecules are either bound to or in close proximity to MNPs rotating within non-heating low-frequency ($f < 1$ kHz) AMF[49]. This can cause changes in the mechanical homeostasis within the biological system, thereby inducing apoptosis in cells.

Cell apoptosis, also known as programmed cell death, leads to cell demise, but it is crucial for the sustained health of the entire organism[75]. A common example of regulated cell apoptosis is the individualization of the digit during embryonic development, such as in the formation of fingers and toes. On the other hand, if apoptosis is improperly regulated, uncontrolled cell growth can lead to fibrosis and tumour formation, while excessive apoptosis can lead to degenerative diseases. In fact, a hallmark of cancer is the ability of malignant cells to evade apoptosis[76].

There are many environmental factors that can trigger cell apoptosis, such as pH, oxygen levels, and inflammatory signalling molecules. it is increasingly recognised that the mechanical environment is also a key factor of cell apoptosis. Altering the mechanical homeostasis inside and outside the cell through mechanical stimulation can induce cell apoptosis. How cells translate mechanical stimuli into apoptotic responses is an active area of research in cellular mechanobiology[76]. Currently, there is no clear mechanism for how mechanical stimuli initiate cell apoptosis. Most studies can only correlate mechanical stimulation with observed cellular responses. For instance, elevated mechanical stress has been shown to induce cell apoptosis by causing excessive DNA damage. As for the mechanisms by which mechanical stimulation regulates cell apoptosis, a widely accepted hypothesis is that mechanical stimuli can induce ion transport across transmembrane ion channels. The influx of calcium and chloride ions has been shown to activate caspases and subsequent cell apoptosis[77].

In this experiment, it is hypothesized that the mechanical stimulation induced by MNPs leads to lysosomal membrane permeabilization, causing the release of hydrolytic enzymes from lysosomes into the cytoplasm, leading to cell apoptosis and cell death[78]. Lysosomes are single-membrane vesicular structures containing various acidic hydrolytic enzymes. The internal pH of lysosomes is low, around 4.5–5.5. This low pH is conducive to the degradation of contaminants that canbe internalized from the external environment by endocytosis, forming vesicles. The fusion of primary lysosomes with the outer membrane of vesicles forms secondary lysosomes, releasing hydrolytic enzymes to degrade their contents, thereby eliminating contaminants. The consumption of lysosomes also has corresponding pathways for lysosome regeneration to ensure their recycling[59, 76]. Therefore, the intact permeability of lysosomal membranes is crucial for the life and

death of cells.

The energy generated by LF-AMF and MNPs is largely the shear stress generated by the rotation of the MNPs, which may cause significant damage to the lysosomal membrane. When cells internalize MNPs through endocytosis, the increased concentration of MNPs results in greater shear force, potentially leading to cell apoptosis. This effect is particularly notable for macrophages, where lysosomes are a key cellular organelle. Another possibility is that the NMMA effect induced by LF-AMF itself has the ability to alter the permeability of the cell membrane[73]. This is supported by TEM observations showing the accumulation of some MNPs close to the cell membrane.

In this experiment, under the conditions of a 10 Hz frequency and a magnetic flux of 160 mT, the alternating magnetic field did not induce significant changes in cell viability and morphology in the absence of PAA. This observation suggests that the sole effect of NMMA does not trigger cellular apoptosis. However, upon the introduction of PAA at a concentration of 75 μg/mL, significant cell damage was observed when the magnetic field was applied. As mentioned earlier, the introduction of MNPs can induce alterations in the mechanical homeostasis within biological systems, consequently leading to cell apoptosis. The selection of the concentration of 75 μg/mL was based on the findings of MNPs toxicity experiments, where excessively high concentrations were found to directly induce cell death.

5.3. Comparisons with other treatments

Nowadays, there are many treatments for obesity, each of which has different advantages and disadvantages. The more common ones are diet, exercise, pharmacological treatment and surgery[79].

5.3.1. Comparisons with some conventional treatments without MNPs

Diet and exercise

Although dieting can achieve weight loss and a thinner physique within a relatively short timeframe, prolonged dieting without medical guidance can lead to undesirable consequences. Diet and weight loss can impact an individual's hair, particularly when the intake of fat and protein is severely restricted during the weight loss process, resulting in hair loss and a gradual loss of hair lustre[80]. One of the more severe outcomes is the potential development of osteoporosis, especially in women. Many women who embark on weight loss diets may experience insufficient oestrogen levels in their bodies, which can disrupt calcium absorption and bone metabolism, ultimately leading to reduced normal bone density and an elevated risk of osteoporosis. Another popular dietary approach is known as low-calorie ketogenic diets (VLCKD). However, the precise mechanisms of weight loss associated with VLCKD remain unclear. And improper VLCKD also can lead to malnutrition, significant loss of strength and energy, and even fainting. Most importantly, they can traverse the blood-brain barrier, entering the nervous system and causing damage, resulting in impaired judgment[81, 82]. The European Association for the Study of Obesity emphasizes that VLCKD should only be used as part of a comprehensive plan under the supervision of obesity experts or other nutritionally trained physician[83].

Exercise represents a highly challenging approach to weight management, necessitating prolonged, continuous physical activity, and frequently adjusted dietary plans. However, it often yields the most favourable outcomes. Its underlying principle aligns with that of diet-induced weight loss, aiming to create an energy deficit by expending more energy than is absorbed. However, exercise places a greater emphasis on energy expenditure, particularly targeting the utilization of fat stored within adipocytes. Some studies also suggest that exercise can stimulate the consumption of fat by BAT[84]. Although these approaches do not typically reduce the quantity of adipocytes, controlling daily energy intake, maintaining a balance between energy expenditure and intake, and fostering a routine exercise regimen emerge as a superior choice compared to mere dietary restriction. Furthermore, these practices offer significant health benefits[17]. An important observation pertains to the challenge of sustaining weight loss attained through dietary adjustments and consistent physical exercise. It is not unusual for individuals to encounter weight regain upon discontinuation of their dietary or exercise regimen. This phenomenon underscores the complex interplay between ongoing physical activity and weight control, underscoring that the cessation of exercise can rapidly result in a reoccurrence of obesity.

Pharmacological treatments

Pharmacological treatments can be classified mainly into two categories, depending on if the drug modifies the appetite acting or not at the central nervous system.

Drugs that act on the central nervous system:

The main action of these drugs is on 5-hydroxytryptamine (5-HT; serotonin), which can increase satiety and decreases appetite. **Fenfluramine** is a serotoninergic medication that was used as an appetite suppressant for the treatment of obesity in the seventies. The precise mechanism by which potentiation of serotonergic transmission by fenfluramine results in appetite suppression involves stimulation of 5-HT_{1B}, 5-HT_{2C} and possibly 5-HT_{2B} receptors, an indirect effect resulting from interaction with the serotonin transporter (SERT) and subsequent inhibition of 5-HT uptake and stimulation of 5-HT release[85]. But fenfluramine was found to be associated with primary pulmonary hypertension and cardiac valvopathy, which led to their withdrawal in 1997[86]. **Fluoxetine** is an antidepressant drug that also acts on 5-HT, which has a slight effect on the appetite and weight of the user, and can be used in obese patients with depression[87]. **Sibutramine** is a serotonin and noradrenaline re-uptake inhibitor (SNRI) which induces weight loss via a dual mode of action, enhancing both satiety and energy expenditure reducing visceral fat effectively. Sibutramine is well tolerated, and its side-effects are generally mild. Overall, studies have found sibutramine to be an effective weight loss agent with a good safety profile[88].

Non-central nervous system drugs:

Orlistat (Xenical®) works by inhibiting gastrointestinal and pancreatic lipases. It blocks the hydrolysis of triglycerides decreasing the absorption of fatty acids carried out at the intestine. This mechanism blocks the absorption of approximately one-third of the fatty acids consumed with food. As a result, it reduces calories absorption without affecting the appetite. Considering its mechanism of action, orlistat seems to be more suitable for those patients who tend to eat fatty food where the drug may have a greater weight-loss effect than in those with non-fatty food consumption habits[89, 90]. But Orlistat also has significant side effects, mainly related to gastrointestinal adverse events. because of the non-absorbed fats in the intestine, patients can experience steatorrhea, frequent bowel movements, flatus with discharge, and faecal incontinence. These gastrointestinal adverse events are generally decreased in frequency with ongoing orlistat treatment[91]. Another class of hormone-based medications, known as glucagon-like peptide-1 receptor agonists

(GLP-1RAs), includes common drugs like **liraglutide** (Victoza®, Xultophy® and Saxenda®) and **semaglutide** (Ozempic® and Wegovy®)[92-94]. These medications have the ability to promote insulin secretion in a glucose-dependent manner. Their mechanism of action as weight loss drugs involves the inhibition of gastrointestinal motility and gastric acid secretion, leading to a delay in gastric emptying. This, in turn, suppresses appetite and food intake.

Surgery

Obesity surgery can be categorized into two approaches: those that restrict food intake and those that reduce the number of adipocytes. Bariatric surgery offers a clear path to short-term weight reduction, boasting a notably high long-term satisfaction rate. Its current status as the sole enduringly effective treatment for obesity primarily stems from its fundamental control over issues related to excessive food intake and nutrient absorption, notwithstanding potential instances of nutritional malabsorption in some patients. Postoperatively, under the guidance of healthcare professionals, patients can maintain a stable and healthy weight range over an extended duration.

One of the earliest surgical procedures employed to treat obesity was jejunoileal bypass. This is a surgical procedure in which most of the small intestine is bypassed, limiting the ability of the patient to digest and absorb nutrients, regardless of the quantity consumed. This approach, however, resulted in severe and enduring health complications, including nutrient deficiencies, and has since been discontinued. Nevertheless, in response to the ongoing demand for weight loss procedures, alternative techniques that primarily emphasize gastric restriction and minimize malabsorption have been developed. Among the most performed bariatric surgeries today are the Roux-en-Y gastric bypass and the adjustable gastric band[95]. The mortality rate associated with laparoscopic Roux-en-Y gastric bypass is approximately 0.1%, with an incidence of severe early complications at 5%. Long-term follow-up data of laparoscopic Roux-en-Y gastric bypass reveals that for the majority of patients, weight loss typically averages 65%, with over 85% of them achieving and sustaining a 50% reduction in their initial excess weight[96].

Liposuction, medically known as suction-assisted lipectomy, ranks as the second most performed surgical procedure in America. It primarily focuses on the removal of fat tissue from the subcutaneous space, primarily serving as a 'cosmetic procedure' rather than a means for significant weight loss[95, 96]. While liposuction can lead to short-term weight reduction, it does not offer a permanent solution to obesity. In the absence of proper medical guidance, some individuals, driven by cosmetic preferences, may excessively extract fat. This can trigger counterregulatory responses, resulting in hypertrophy and hyperplasia of adipocytes[97].

In summary, obesity represents a chronic and progressive condition influenced by various environmental and genetic factors, necessitating lifelong management. When lifestyle modifications fail to effectively control weight, pharmaceutical interventions are often prescribed. If pharmaceutical treatments successfully manage weight without significant adverse effects, they are administered continuously. Given the elevated health risks associated with obesity-related morbidity and mortality in many patients, pharmacological approaches should be considered for obesity management. The incorporation of MNPs into obesity treatment, either as a standalone therapeutic approach or in combination with various other drugs, remains a significant avenue for future development in nanomedicine. While studies exploring the potential interactions of MNPs with other drugs in combination therapy are currently limited, their immense potential cannot be underestimated. It is believed that the combined use of MNPs with other drugs in treatment holds considerable promise and may emerge as an effective obesity management approach comparable to surgical interventions[98].

5.3.2. Comparisons with other treatments also using MNPs

Compared to NMMA, there is another more widely used treatment for MNPs. Magnetic targeted hyperthermia (MTH) represents an alternative approach to cancer treatment using MNPs. Hyperthermia is a therapeutic approach that aims to raise the temperature of cancerous regions of the body to 40-43°C. However, as a stand-alone treatment, hyperthermia is ineffective and is typically used to enhance the cytotoxicity of radiotherapy and chemotherapy, inducing cancer cell death. A major drawback of traditional hyperthermia is that, in general, both malignant and non-malignant cells exhibit

similar sensitivity to heating[99]. However, MTH involves the introduction of MNPs into the targeted site, followed by the application of an alternating magnetic field with the objective of raising the temperature of the targeted area to over 41°C[100]. There is evidence that certain types of cancers, including glioblastoma cells, can uptake magnetic nanoparticles more effectively than non-malignant cells[101]. MTH works by converting magnetic energy into heat energy within an oscillating magnetic field. The achieved temperature can be precisely regulated by adjusting the amplitude and frequency of these oscillations.

Magnetic fields utilized in MTH typically range from 1 KHz to 1 MHz, which is much higher than the magnetic field frequency used in NMMA [102].

In fact, high-frequency alternating magnetic fields are harmful to the human body. Over 95% of the human body is composed of conductive materials, including electrolytes within the body. Under the influence of high-frequency alternating magnetic fields, eddy currents can form in the conductive tissues of the body, leading to damage. Moreover, certain extremely high-intensity frequencies can induce mental disorders, heart rhythm abnormalities, and even directly trigger phenomena like atrial fibrillation, posing significant dangers[103]. While MTH has been partially employed as an alternative to conventional treatments, it is still primarily restricted to temperature-sensitive cells, such as those in cancer therapy. There is currently no well-established solution for regular cells like adipocytes. Additionally, due to the temperature elevation associated with MTH, there are increased demands on the outer coatings of MNPs compared to NMMA[72]. Firstly, the stability of the outer coating of MNPs is closely related to the heating environment and is temperature-dependent. In order to generate a high-temperature environment, there is a significant requirement for the connection between the outer coating and the nanometallic core due to the enormous shear stress generated by the rapid movement of MNPs in a high-frequency alternating magnetic field. Therefore, ensuring appropriate chemical stability and biocompatibility while generating a substantial amount of heat for thermal therapy places much greater demands on the outer coating compared to NMMA technology[104]. In conclusion, the high-frequency alternating magnetic field itself poses potential hazards to the human body and may lead to instability in surface coatings under elevated temperatures. These aspects highlight the limitations of MTH compared to the therapeutic efficacy of NMMA effects.

In addition to the commonly employed magnetic hyperthermia, various other therapeutic modalities utilize high-frequency magnetic fields, each with its own merits and drawbacks. For instance, physical therapy using ultrahigh frequency in the range of 26–40 MHz and transcranial magnetic stimulation within the frequency range of 1–10 kHz are two such methods that do not require the introduction of MNPs. However, the former is associated with excessively high and potentially unsafe magnetic field frequencies, while the latter, due to its non-specificity, lacks precise localization of the treatment area[49].

Compared to the aforementioned weight loss methods, the nano-magnetic field treatment targeting obesity-related macrophages in this experiment represents a novel, rigorously controlled, and nearly harmless therapeutic approach. Rather than directly targeting adipocytes, this method indirectly addresses obesity by controlling the transformational relationship between macrophages and white or beige adipocytes. This approach not only treats obesity but may also have preventive effects. The use of LF-AMF in conjunction with NMMA in the experiment demonstrated its remarkable efficacy, and the toxicity concentration tests confirmed the safety and appropriateness of the treatment concentration in the relevant magnetic nanoparticles, particularly those containing PAA.

6. Conclusion

This study examined several characteristics of novel surface-coated MNPs, including size, zeta potential, blood compatibility, and cytotoxicity. The results indicate that standalone MNPs can indeed induce hemolysis and cell death in the short term when present at high concentrations. The potential cause of cell death may be attributed to lysosomal degradation, leading to the exposure of the highly toxic metal core of MNPs. Furthermore, MNPs exhibited varying characteristics in different media, such as an increase in size and a decrease in stability. Therefore, additional research is needed to further understand and investigate the surface coatings of MNPs.

Subsequently, this study discusses and summarizes the therapeutic applications of MNPs on macrophages under the influence of LF-AMF utilizing the NMMA effect. The results indicate that readily attainable and safe LF-AMF can successfully induce cell apoptosis, achieving the desired therapeutic effects with MNPs.

This approach provides a reliable tool for altering enzyme activity, addressing drug delivery, and controlling techniques related to conventional non-tumour cells. It offers a solid foundation and broad prospects for the next generation of therapies, which, compared to existing methods, are safer with fewer side effects. To implement this strategy in medical practice, further theoretical and biochemical experiments are needed before transitioning from the laboratory to clinical settings.

As the application of nanotechnology continues to expand, the impact of MNPs on cells and animal models needs to keep pace. In this experiment, only haemolysis tests, exploration of potential effects on platelets, and toxicity testing at different concentrations of MNPs were conducted. However, a comprehensive toxicological analysis of MNPs is essential to identify the key physical or chemical properties of MNPs that contribute to their toxicity. This analysis aids in designing safer strategies by optimizing their physicochemical properties to minimize MNPs toxicity while maximizing their biological efficacy. This can be achieved by directly developing MNPs with lower toxicity or exploring outer coatings with higher biocompatibility, such as the different types of MNPs used in this experiment.

7. Future work

We have shown that LF-AMF using non-targeted nanoparticles can induce macrophage death. Therefore, if we use targeted nanoparticles, this technology could potentially be used to modify the permeability of cell membranes associated with lipid droplet storage in adipocytes, thereby facilitating the removal of excess triglycerides without causing the death of other cell types present in AT. Achieving this requires precise control of the nanoparticles and the magnetic field. In addition, as the MNPs in this experiment acted on macrophages, adjusting the properties of the MNPs to only affect adipocytes is a potential avenue for future research. The toxicology of nanoparticles cannot be overlooked, and a more realistic simulation of the actual cellular environment is an important direction for the development of MNPs specifically for adiposopathy. The diversification and intelligent design of MNPs by adjusting their inherent properties and targeting moieties, in combination with externally controlled and precise magnetic fields, may enable them to achieve effects like the medical nanorobots of science fiction. Moving the experiment from the laboratory to the clinic to validate safety and efficacy in the human body is a crucial next step.

In future studies, we expect to further investigate the therapeutic mechanisms of nanoparticles activated by low frequency alternating magnetic fields on adipocytes. A full understanding is essential to realise the potential applications of these techniques in the treatment of adiposopathy and related diseases. We hope that this research will contribute to the development of innovative treatment strategies and address obesity-related health issues. Future developments in this area promise to provide patients with safer and more effective treatment options for obesity,

Acknowledgements

We also acknowledge those who donated blood samples for this research. And the people who worked with me, Anushka Kulkarni, Giorgia Papini, Saoirse Morrin, Tiina O'Neill.

References

1. Caballero, B., *Humans against Obesity: Who Will Win?* Adv Nutr, 2019. **10**(suppl_1): p. S4-S9.
2. Mathew M Avram 1, A.S.A., William D James, *Subcutaneous fat in normal and diseased states 3. Adipogenesis: from stem cell to fat cell.* Journal of the American Academy of Dermatology, 2007 Mar. **56**(3).
3. Ghaben, A.L. and P.E. Scherer, *Adipogenesis and metabolic health.* Nature Reviews Molecular Cell Biology, 2019. **20**(4): p. 242-258.
4. Rothman, K.J., *BMI-related errors in the measurement of obesity.* International Journal of Obesity, 2008. **32**(S3): p. S56-S59.
5. Lemos, T. and D. Gallagher, *Current body composition measurement techniques.* Current Opinion in Endocrinology & Diabetes and Obesity, 2017. **24**(5): p. 310-314.
6. Frigolet, M.E. and R. Gutiérrez-Aguilar, *The colors of adipose tissue.* Gaceta Médica de México, 2023. **156**(2).
7. Caslin, H.L., et al., *Adipose tissue macrophages: Unique polarization and bioenergetics in obesity.* Immunological Reviews, 2020. **295**(1): p. 101-113.
8. Li, B., et al., *Adipose tissue macrophages: implications for obesity-associated cancer.* Military Medical Research, 2023. **10**(1).
9. Jonathan and D. Artis, *Immune Regulation of Metabolic Homeostasis in Health and Disease.* Cell, 2015. **161**(1): p. 146-160.
10. Xiaoyan Hui 1, P.G., Jialiang Zhang 1, Tao Nie 3, Yong Pan 1, Donghai Wu 3, Tianshi Feng 1, Cheng Zhong 1, Yu Wang 4, Karen S L Lam 1, Aimin Xu *Adiponectin Enhances Cold-Induced Browning of Subcutaneous Adipose Tissue via Promoting M2 Macrophage Proliferation.* Cell Metab, 2015. **22**(2): p. P279-290.
11. Gao, D., et al., *Interleukin-1β mediates macrophage-induced impairment of insulin signaling in human primary adipocytes.* Am J Physiol Endocrinol Metab, 2014. **307**(3): p. E289-304.
12. Zhuge, F., et al., *DPP-4 Inhibition by Linagliptin Attenuates Obesity-Related Inflammation and Insulin Resistance by Regulating M1/M2 Macrophage Polarization.* Diabetes, 2016. **65**(10): p. 2966-2979.
13. *"World Health Organization"*. Available from: https://www.who.int/.
14. *"National Health and Nutrition Examination Survey"*. Available from: https://www.cdc.gov/nchs/nhanes/index.htm.
15. *Eurostat.*
16. Jia, P., et al., *Fast-food restaurant, unhealthy eating, and childhood obesity: A systematic review and meta-analysis.* Obesity Reviews, 2021. **22**(S1).
17. Swift, D.L., et al., *The Effects of Exercise and Physical Activity on Weight Loss and Maintenance.* Prog Cardiovasc Dis, 2018. **61**(2): p. 206-213.
18. Kolotkin, R.L., K. Meter, and G.R. Williams, *Quality of life and obesity.* Obesity Reviews, 2001. **2**(4): p. 219-229.
19. Pi-Sunyer, F.X., *The Obesity Epidemic: Pathophysiology and Consequences of Obesity.* Obesity Research, 2002. **10**(S12): p. 97S-104S.
20. Hampl, S. and A. Campbell, *Recognizing obesity and its complications: the story of Score 1 for Health.* NASN Sch Nurse, 2015. **30**(1): p. 46-52.
21. Seravalle, G. and G. Grassi, *Corrigendum to "Obesity and hypertension" [Pharmacol. Res. 122 (2017) 1-7].* Pharmacol Res, 2017. **124**: p. 156.
22. Conway, B. and A. Rene, *Obesity as a disease: no lightweight matter.* Obesity Reviews, 2004. **5**(3): p. 145-151.

23. Lu, B., et al., *Adipose tissue macrophages in aging-associated adipose tissue function.* The Journal of Physiological Sciences, 2021. **71**(1): p. 38.
24. Tiwari, P., et al., *Metabolically activated adipose tissue macrophages link obesity to triple-negative breast cancer.* J Exp Med, 2019. **216**(6): p. 1345-1358.
25. Liang, Y., et al., *Elevated IL-33 promotes expression of MMP2 and MMP9 via activating STAT3 in alveolar macrophages during LPS-induced acute lung injury.* Cell Mol Biol Lett, 2018. **23**: p. 52.
26. Jiang, H. and H. Li, *Prognostic values of tumoral MMP2 and MMP9 overexpression in breast cancer: a systematic review and meta-analysis.* BMC Cancer, 2021. **21**(1): p. 149.
27. Bayda, S., et al., *The History of Nanoscience and Nanotechnology: From Chemical–Physical Applications to Nanomedicine.* Molecules, 2019. **25**(1): p. 112.
28. Contera, S., J. Bernardino de la Serna, and T.D. Tetley, *Biotechnology, nanotechnology and medicine.* Emerg Top Life Sci, 2020. **4**(6): p. 551-554.
29. Yohan, D. and B.D. Chithrani, *Applications of nanoparticles in nanomedicine.* J Biomed Nanotechnol, 2014. **10**(9): p. 2371-92.
30. Hofmann-Amtenbrink, M., H. Hofmann, and X. Montet, *Superparamagnetic nanoparticles - a tool for early diagnostics.* Swiss Medical Weekly, 2010.
31. Baetke, S.C., T. Lammers, and F. Kiessling, *Applications of nanoparticles for diagnosis and therapy of cancer.* The British Journal of Radiology, 2015. **88**(1054): p. 20150207.
32. Mitchell, M.J., et al., *Engineering precision nanoparticles for drug delivery.* Nature Reviews Drug Discovery, 2021. **20**(2): p. 101-124.
33. *Current approaches of nanomedicines in the market and various stage of clinical translation.* Acta Pharmaceutica Sinica B, uly 2022. **12**(7): p. 3028-3048.
34. Joy Wolfram a b, M.F.b.c., *Clinical cancer nanomedicine.* Nano Today, April 2019. **25**: p. 85-98.
35. Kim, J., et al., *Perspectives for Improving the Tumor Targeting of Nanomedicine via the EPR Effect in Clinical Tumors.* International Journal of Molecular Sciences, 2023. **24**(12): p. 10082.
36. Danhier, F., *To exploit the tumor microenvironment: Since the EPR effect fails in the clinic, what is the future of nanomedicine?* Journal of Controlled Release, 28 December 2016,. **244**: p. 108-121.
37. Kumari, M. and S.K. Gupta, *Removal of aromatic and hydrophobic fractions of natural organic matter (NOM) using surfactant modified magnetic nanoadsorbents (MNPs).* Environmental Science and Pollution Research, 2018. **25**(25): p. 25565-25579.
38. Alkilany, A.M., et al., *Ligand density on nanoparticles: A parameter with critical impact on nanomedicine.* Adv Drug Deliv Rev, 2019. **143**: p. 22-36.
39. Lewinski, N., V. Colvin, and R. Drezek, *Cytotoxicity of Nanoparticles.* Small, 2008. **4**(1): p. 26-49.
40. Najahi-Missaoui, W., R.D. Arnold, and B.S. Cummings, *Safe Nanoparticles: Are We There Yet?* International Journal of Molecular Sciences, 2020. **22**(1): p. 385.
41. William W Yu1, Emmanuel Chang2, Christie M Sayes1,Rebekah Drezek2and Vicki L Colvin, *Aqueous dispersion of monodispersemagnetic iron oxide nanocrystals throughphase transfer.* Nanotechnology17(2006) 4483–4487, 21 August 2006.
42. Yuan, J., E. Peng, and J.M. Xue, *Controlled loading of paramagnetic gadolinium oxide nanoplates in PMAO-g-PEG as effective T₁-weighted MRI contrast agents.* Journal of Materials Research, 2014. **29**(15): p. 1626-1634.
43. Jincan He, M.H., Dongmei Wang, Zhuomin Zhang, Gongke Li, *Magnetic separation techniques in sample preparation for biological analysis: A review.* Journal of Pharmaceutical and Biomedical Analysis, December 2014. **101**: p. 84-101.

44. Qinyue Gao, J.Z., Jie Gao, Zhengyang Zhang, Haitao Zhu, and Dongqing Wang*, *Gold Nanoparticles in Cancer Theranostics.* Front Bioeng Biotechnol, 2021 Apr 13. **9**.
45. Gobbo, O.L., et al., *Magnetic Nanoparticles in Cancer Theranostics.* Theranostics, 2015. **5**(11): p. 1249-1263.
46. Zang, X., et al., *Nanoparticles for tumor immunotherapy.* Eur J Pharm Biopharm, 2017. **115**: p. 243-256.
47. Chen, L., et al., *A Redox-Sensitive Micelle-Like Nanoparticle Self-Assembled from Amphiphilic Adriamycin-Human Serum Albumin Conjugates for Tumor Targeted Therapy.* BioMed Research International, 2015. **2015**: p. 1-10.
48. Zhang, Y., et al., *Versatile metal-phenolic network nanoparticles for multitargeted combination therapy and magnetic resonance tracing in glioblastoma.* Biomaterials, 2021. **278**: p. 121163.
49. Golovin, Y.I., et al., *Non-Heating Alternating Magnetic Field Nanomechanical Stimulation of Biomolecule Structures via Magnetic Nanoparticles as the Basis for Future Low-Toxic Biomedical Applications.* Nanomaterials, 2021. **11**(9): p. 2255.
50. Santos-Martínez, M.J., et al., *Analysis of platelet function: role of microfluidics and nanodevices.* Analyst, 2011. **136**(24): p. 5120-6.
51. Clogston, J.D. and A.K. Patri, *Zeta potential measurement.* Methods Mol Biol, 2011. **697**: p. 63-70.
52. King, R.A.N., et al., *A Human Erythrocyte-based Haemolysis Assay for the Evaluation of Human Complement Activity.* Altern Lab Anim, 2020. **48**(3): p. 127-135.
53. sigmaaldrich, *Cell Counting Kit – 8.*
54. Strober, W., *Trypan Blue Exclusion Test of Cell Viability.* Curr Protoc Immunol, 2015. **111**: p. A3.B.1-a3.B.3.
55. Medina, C., et al., *Platelet aggregation-induced by caco-2 cells: regulation by matrix metalloproteinase-2 and adenosine diphosphate.* J Pharmacol Exp Ther, 2006. **317**(2): p. 739-45.
56. Couto, D., et al., *Biodistribution of polyacrylic acid-coated iron oxide nanoparticles is associated with proinflammatory activation and liver toxicity.* J Appl Toxicol, 2016. **36**(10): p. 1321-31.
57. Gupta, A.K. and M. Gupta, *Synthesis and surface engineering of iron oxide nanoparticles for biomedical applications.* Biomaterials, 2005. **26**(18): p. 3995-4021.
58. Murdock, R.C., et al., *Characterization of nanomaterial dispersion in solution prior to in vitro exposure using dynamic light scattering technique.* Toxicol Sci, 2008. **101**(2): p. 239-53.
59. Marcano, L., et al., *Magnetic Anisotropy of Individual Nanomagnets Embedded in Biological Systems Determined by Axi-asymmetric X-ray Transmission Microscopy.* ACS Nano, 2022. **16**(5): p. 7398-7408.
60. Liao, C., Y. Li, and S.C. Tjong, *Bactericidal and Cytotoxic Properties of Silver Nanoparticles.* Int J Mol Sci, 2019. **20**(2).
61. Everts, P.A., et al., *Platelet-rich plasma and platelet gel: a review.* J Extra Corpor Technol, 2006. **38**(2): p. 174-87.
62. Baaten, C.C.F.M.J., et al., *Platelet populations and priming in hematological diseases.* Blood Reviews, 2017. **31**(6): p. 389-399.
63. Sharma, A., S.V. Madhunapantula, and G.P. Robertson, *Toxicological considerations when creating nanoparticle-based drugs and drug delivery systems.* Expert Opin Drug Metab Toxicol, 2012. **8**(1): p. 47-69.
64. Zhang, B.B., et al., *Lipid/PAA-coated mesoporous silica nanoparticles for dual-pH-responsive codelivery of arsenic trioxide/paclitaxel against breast cancer cells.* Acta Pharmacol Sin, 2021. **42**(5): p. 832-842.

65. Soenen, S.J., et al., *The role of nanoparticle concentration-dependent induction of cellular stress in the internalization of non-toxic cationic magnetoliposomes.* Biomaterials, 2009. **30**(36): p. 6803-13.
66. Fang, C.Y., et al., *Long-term growth comparison studies of FBS and FBS alternatives in six head and neck cell lines.* PLoS One, 2017. **12**(6): p. e0178960.
67. Yang, X., et al., *A simple colorimetric method for viable bacteria detection based on cell counting Kit-8.* Anal Methods, 2021. **13**(43): p. 5211-5215.
68. Nemmar, A., et al., *Oxidative stress, inflammation, and DNA damage in multiple organs of mice acutely exposed to amorphous silica nanoparticles.* Int J Nanomedicine, 2016. **11**: p. 919-28.
69. Franklin, N.M., et al., *Comparative toxicity of nanoparticulate ZnO, bulk ZnO, and ZnCl2 to a freshwater microalga (Pseudokirchneriella subcapitata): the importance of particle solubility.* Environ Sci Technol, 2007. **41**(24): p. 8484-90.
70. Li, B., et al., *Adipose tissue macrophages: implications for obesity-associated cancer.* Mil Med Res, 2023. **10**(1): p. 1.
71. Batista-Gonzalez, A., et al., *New Insights on the Role of Lipid Metabolism in the Metabolic Reprogramming of Macrophages.* Front Immunol, 2019. **10**: p. 2993.
72. Xu, X., et al., *Obesity activates a program of lysosomal-dependent lipid metabolism in adipose tissue macrophages independently of classic activation.* Cell Metab, 2013. **18**(6): p. 816-30.
73. Richard H.W. Funk, T.M., Nurdan Özkucur, *Electromagnetic effects – From cell biology to medicine.* Progress in Histochemistry and Cytochemistry, February 2009, . **Volume 43,**(4): p. Pages 177-264.
74. Buchachenko, A., *Why magnetic and electromagnetic effects in biology are irreproducible and contradictory?* Bioelectromagnetics, 2016. **37**(1): p. 1-13.
75. Clark, R.S., et al., *Increases in Bcl-2 and cleavage of caspase-1 and caspase-3 in human brain after head injury.* Faseb j, 1999. **13**(8): p. 813-21.
76. Goldblatt, Z.E., H.A. Cirka, and K.L. Billiar, *Mechanical Regulation of Apoptosis in the Cardiovascular System.* Ann Biomed Eng, 2021. **49**(1): p. 75-97.
77. Bortner, C.D. and J.A. Cidlowski, *Ion channels and apoptosis in cancer.* Philos Trans R Soc Lond B Biol Sci, 2014. **369**(1638): p. 20130104.
78. Mahapatra, K.K., et al., *The lysosome as an imperative regulator of autophagy and cell death.* Cellular and Molecular Life Sciences, 2021. **78**(23): p. 7435-7449.
79. Warrier, G. and M.A. Incze, *I Want to Lose Weight: Which Diet Is Best?* JAMA Internal Medicine, 2021. **181**(9): p. 1268.
80. Guo, E.L. and R. Katta, *Diet and hair loss: effects of nutrient deficiency and supplement use.* Dermatology Practical & Conceptual, 2017: p. 1-10.
81. Hall, K.D., D.A. Schoeller, and A.W. Brown, *Reducing Calories to Lose Weight.* JAMA, 2018. **319**(22): p. 2336.
82. Basolo, A., et al., *Ketogenic Diet and Weight Loss: Is There an Effect on Energy Expenditure?* Nutrients, 2022. **14**(9): p. 1814.
83. Muscogiuri, G., et al., *The management of very low-calorie ketogenic diet in obesity outpatient clinic: a practical guide.* Journal of Translational Medicine, 2019. **17**(1).
84. Cheng, L., et al., *Brown and beige adipose tissue: a novel therapeutic strategy for obesity and type 2 diabetes mellitus.* Adipocyte, 2021. **10**(1): p. 48-65.
85. Odi, R., et al., *Fenfluramine repurposing from weight loss to epilepsy: What we do and do not know.* Pharmacol Ther, 2021. **226**: p. 107866.
86. Connolly, H.M., et al., *Valvular Heart Disease Associated with Fenfluramine–Phentermine.* New England Journal of Medicine, 1997. **337**(9): p. 581-588.
87. Tao R, F.A., Aspley S, Brammer R, Heal D, Auerbach S., *Effects on serotonin in rat hypothalamus of D-fenfluramine, aminorex, phentermine and fluoxetine.* Eur J Pharmacol., 2002 Jun 7. **445(1-2)**: p. 69-81.

88. Van Gaal LF, W.M., De Leeuw IH., *Anti-obesity drugs: what does sibutramine offer? An analysis of its potential contribution to obesity treatment.* Exp Clin Endocrinol Diabetes, 1998. **106 Suppl 2**: p. 35-40.
89. Ballinger, A., *Orlistat in the treatment of obesity.*
90. Heck, A.M., J.A. Yanovski, and K.A. Calis, *Orlistat, a New Lipase Inhibitor for the Management of Obesity.* Pharmacotherapy, 2000. **20**(3): p. 270-279.
91. Filippatos, T.D., et al., *Orlistat-Associated Adverse Effects and Drug Interactions.* Drug Safety, 2008. **31**(1): p. 53-65.
92. Wilding, J.P.H., et al., *Once-Weekly Semaglutide in Adults with Overweight or Obesity.* New England Journal of Medicine, 2021. **384**(11): p. 989-1002.
93. Lundgren, J.R., et al., *Healthy Weight Loss Maintenance with Exercise, Liraglutide, or Both Combined.* New England Journal of Medicine, 2021. **384**(18): p. 1719-1730.
94. Onakpoya, I.J., et al., *Naltrexone–bupropion (Mysimba) in management of obesity: A systematic review and meta-analysis of unpublished clinical study reports.* British Journal of Clinical Pharmacology, 2020. **86**(4): p. 646-667.
95. Genser, L., et al., *Laparoscopic Roux-en-Y gastric bypass with hand-sewn gastro-jejunostomy.* J Visc Surg, 2017. **154**(1): p. 37-45.
96. Madura, J.A. and J.K. Dibaise, *Quick fix or long-term cure? Pros and cons of bariatric surgery.* F1000 Medicine Reports, 2012. **4**.
97. Vogt, T., & Belluscio, D. , *Controversies in plastic surgery: Suction-assisted lipectomy (SAL) and the hCG (human chorionic gonadotropin) protocol for obesity treatment.* . Aesthetic Plastic Surgery, 1987. **11(1)**: p. 131–156.
98. Tak, Y.J. and S.Y. Lee, *Long-Term Efficacy and Safety of Anti-Obesity Treatment: Where Do We Stand?* Current Obesity Reports, 2021. **10**(1): p. 14-30.
99. Chang, D., et al., *Biologically Targeted Magnetic Hyperthermia: Potential and Limitations.* Frontiers in Pharmacology, 2018. **9**.
100. Jose, J., et al., *Magnetic nanoparticles for hyperthermia in cancer treatment: an emerging tool.* Environmental Science and Pollution Research, 2020. **27**(16): p. 19214-19225.
101. Jordan, A., et al., *Inductive heating of ferrimagnetic particles and magnetic fluids: physical evaluation of their potential for hyperthermia.* Int J Hyperthermia, 1993. **9**(1): p. 51-68.
102. Chang, D., et al., *Biologically Targeted Magnetic Hyperthermia: Potential and Limitations.* Front Pharmacol, 2018. **9**: p. 831.
103. Jordan, A., et al., *Presentation of a new magnetic field therapy system for the treatment of human solid tumors with magnetic fluid hyperthermia.* Journal of Magnetism and Magnetic Materials, 2001. **225**(1-2): p. 118-126.
104. Fatima, H., T. Charinpanitkul, and K.-S. Kim, *Fundamentals to Apply Magnetic Nanoparticles for Hyperthermia Therapy.* Nanomaterials, 2021. **11**(5): p. 1203.